AD706693

OAK RIDGE NATIONAL LABORATORY
operated by
UNION CARBIDE CORPORATION
for the
U.S. ATOMIC ENERGY COMMISSION

ORNL-TM-2781

COPY NO. -

DATE - May 7, 1970

Neutron Physics Division

TIME-DEPENDENT NEUTRON AND SECONDARY GAMMA-RAY TRANSPORT IN INFINITE AIR AND IN AIR OVER GROUND

E. A. Straker

Abstract

The general description of the radiation field was determined for several neutron source energies in infinite air and in an air-over-ground geometry for source heights of 50 and 1125 feet. The effect on dose of source height and detector height and the effect of the ground on energy, angular, and time dependence is discussed for both fission and 12.2- to 15-MeV neutron sources. The satisfactory agreement of calculations with experimental results from operations BREN and HENRE and the agreement between Monte Carlo and discrete ordinates results lend confidence to the cross sections used and the computational techniques.

NOTE:

This Work Funded by
DEFENSE ATOMIC SUPPORT AGENCY
Under Subtask No. PB050

Reproduced by the
CLEARINGHOUSE
for Federal Scientific & Technical
Information Springfield Va. 22151

This document has been approved for public release and sale; its distribution is unlimited

DDC
RECEIVED
JUN 4 1970
A

NOTICE This document contains information of a preliminary nature and was prepared primarily for internal use at the Oak Ridge National Laboratory. It is subject to revision or correction and therefore does not represent a final report.

INTRODUCTION

In many shelter design problems it is necessary to know the complete description of the radiation field incident on the shield. That is, it is desirable to know the free-field description of the radiation from a particular weapon spectrum as a function of space, energy, angle, and time. This radiation field also depends on the energy, height, and angular distribution of the source. The neutron and secondary gamma-ray distributions were calculated for several source-energy bands and spectra for source heights of 50 and 1125 ft and for infinite air. The air was considered as homogeneous with a density of 1.11 mg/cc.

Both steady-state and time-dependent calculations were made. In general, the most important time intervals are those in which there are peak intensities. In the problems considered the peaks occurred during the time intervals in which there were fast neutrons. Thus, in most cases the time distribution of the radiation field was determined only for fast neutrons, i.e., with energies greater than 0.1 MeV, and for their secondary gamma rays. In a few calculations the complete time-dependent behavior was determined. In the steady-state calculations the secondary gamma-ray field includes contributions from neutrons of all energies.

Analysis of the calculational results provided information on the effect of source and detector heights on the radiation field, as well as the effect of source energy. Table 1 lists the cases studied.

CALCULATIONAL TECHNIQUES

Both Monte Carlo and discrete ordinates techniques were used to calculate the radiation field. The time dependence of the fast neutrons and their secondary gamma rays was determined with a time-dependent

Table 1. Problems Investigated

Source Energy (MeV)	Source Height (ft)*	Spatial Range (m) for Infinite Air Core
12.2 - 15	50, 1125	0 - 4800
10.0 - 12.2	50	0 - 1800
8.18 - 10.0	50	0 - 1800
6.36 - 8.18	50	0 - 1800
4.06 - 6.36	50	0 - 1800
2.35 - 4.06	50	0 - 1800
1.1 - 2.35	50	0 - 1800
0.11 - 1.11	50	0 - 1800
0.0033 - 0.11	50	0 - 1800
Fission	50, 1125	0 - 4800
Typical thermonuclear	1125	0 - 1800

*Spatial range: 0-1500 m.

version of 05R[1] coupled to a time-dependent version of OGRE.[2] A four-dimensional (space, energy, angle, and time) analysis package[3] was used with ACTIFK[4] for the analysis of the neutron histories, and similar routines were built into a modified version of OGRE. Importance sampling included the exponential transform[5] with an importance function that was symmetrical about the interface in terms of mean free paths and with the importance decreasing with distance from the interface.[6] In addition, gamma-ray source angle biasing as a function of both position and gamma-ray energy were used, as well as Russian roulette and splitting for both neutrons and gamma rays. The neutrons and gamma rays were tracked throughout the air and ground and a flux estimation was made upon leaving each collision based on the particle's probability of crossing the air-ground interface. The technique of Clark[7] was used to remove the infinite variance due to a zero-angle boundary crossing.

Steady-state discrete ordinates calculations for infinite air were made with ANISN,[8] and the results for air over ground were obtained with the two-dimensional code DOT.[9,10] The coupled neutron gamma-ray transport was solved as one problem using a first-collision source to minimize ray effects. Spatial intervals of 30 m for the air were used, except near the source, where smaller intervals were employed.

The air, density 1.11 mg/cc, was assumed to consist of 21% oxygen and 79% nitrogen; the ground was assumed to be 16% hydrogen, 57% oxygen, 19% silicon, and 8% aluminum, at a density of 1.7 g/cc.

The neutron cross sections used in both the Monte Carlo and discrete ordinates results were based on those of ENDF/B except for silicon, which were taken from the 05R Library.[11] To minimize the differences of cross

sections used in the two codes, the fine-group structure for the discrete ordinates calculations was chosen to best represent the detailed structure in the total cross section. These fine-group cross sections (104 groups) were then reduced to 22 neutron groups with ANISN by using the equilibrium energy spectrum in infinite air. The effect of zone weighting was found to be minimal,[12] and a P_3 expansion of the angular distribution of scattering was used for both neutron and gamma rays in the discrete ordinates calculations. The neutron Monte Carlo calculations employed approximately 1000 energy points and a P_8 expansion of the angular distribution.

The gamma-ray-production cross sections were taken from several sources.[13] Tables 2 and 3 give the neutron-to-gamma-ray-transfer cross sections for air and ground, respectively. New gamma-ray-production cross sections have been measured[14,15] for nitrogen and oxygen since these calculations were begun; however, the effects of using these newer cross sections on the results reported here have not been evaluated at this time.

VALIDATION OF METHODS

In order to determine if the cross sections and calculational techniques were reasonable, calculations were made of the neutron and gamma-ray Henderson dose for comparison with experimental results from operations BREN[16-18] and HENRE.[19-21] Figures 1 and 2 show the comparisons of both discrete ordinates and Monte Carlo calculations with measurements of neutron and gamma-ray dose. The agreement is good except for the secondary gamma-ray dose from the BREN experiment. Since the calculated gamma-ray dose is dominated by gamma rays produced by thermal capture in the ground, it is expected that variations in the ground composition

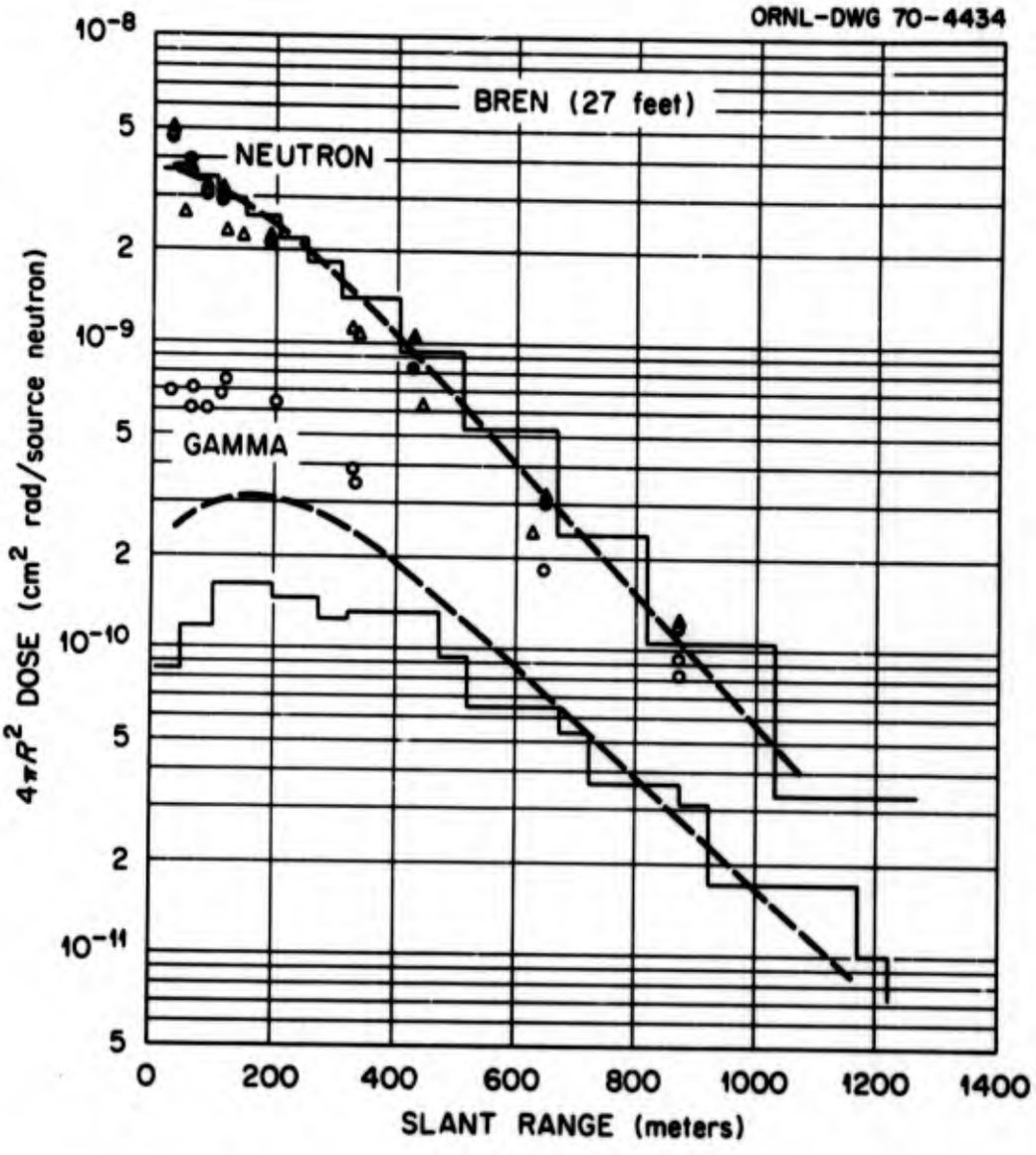

Fig. 1. Comparison of Measured and Calculated Neutron and Secondary Gamma-Ray Doses from the BREN Reactor Operating at 27 ft Above the Ground. Calculations do not include fission gamma rays. —— Monte Carlo; --- Discrete Ordinates; X,Δ ref. 17; 0,0 ref. 18.

Table 2. Gamma-Production Probabilities for Air

Neutron Group Upper Energy (eV)	15.0(+6)*	12.2(+6)	10.0(+6)	8.18(+6)	6.36(+6)	4.96(+6)	4.06(+6)	3.01(+6)	2.46(+6)	2.35(+6)	1.83(+6)
Production Probability	0.669460	0.716140	0.450780	0.253960	0.059958	0.012598	0.003175	0.000891	0.000000	0.000000	0.000000
Gamma Group Upper Energy (eV)	Cumulative Probability										
10.0(+6)	0.0297	0.0193	0.0074	0.0000	0.0000	0.0000	0.0000	0.0000	0.0000	0.0000	0.0000
8.0(+6)	0.1395	0.0943	0.0505	0.0022	0.0000	0.0000	0.0000	0.0000	0.0000	0.0000	0.0000
6.5(+6)	0.3414	0.3147	0.4034	0.2901	0.1839	0.0011	0.0000	0.0000	0.0000	0.0000	0.0000
5.0(+6)	0.4564	0.4220	0.5138	0.4082	0.3025	0.0049	0.0000	0.0000	0.0000	0.0000	0.0000
4.0(+6)	0.5241	0.4935	0.6002	0.6571	0.3201	0.0476	0.0333	0.0000	0.0000	0.0000	0.0000
3.0(+6)	0.6539	0.6189	0.7065	0.7329	0.4627	0.3900	0.5160	0.5000	0.0000	0.0000	0.0000
2.5(+6)	0.6875	0.7490	0.8291	0.8771	0.7739	0.7323	0.9986	1.0000	0.0000	0.0000	0.0000
2.0(+6)	0.7613	0.8314	0.9065	0.9337	0.8781	0.8557	0.9992	1.0000	0.0000	0.0000	0.0000
1.66(+6)	0.8652	0.9328	0.9976	1.0000	1.0000	1.0000	1.0000	1.0000	0.0000	0.0000	0.0000
1.33(+6)	0.9236	0.9603	0.9982	1.0000	1.0000	1.0000	1.0000	1.0000	0.0000	0.0000	0.0000
1.0(+6)	0.9236	0.9603	0.9982	1.0000	1.0000	1.0000	1.0000	1.0000	0.0000	0.0000	0.0000
8.0(+5)	1.0000	1.0000	1.0000	1.0000	1.0000	1.0000	1.0000	1.0000	0.0000	0.0000	0.0000
6.0(+5)	1.0000	1.0000	1.0000	1.0000	1.0000	1.0000	1.0000	1.0000	0.0000	0.0000	0.0000
4.0(+5)	1.0000	1.0000	1.0000	1.0000	1.0000	1.0000	1.0000	1.0000	0.0000	0.0000	0.0000
3.0(+5)	1.0000	1.0000	1.0000	1.0000	1.0000	1.0000	1.0000	1.0000	0.0000	0.0000	0.0000
2.0(+5)	1.0000	1.0000	1.0000	1.0000	1.0000	1.0000	1.0000	1.0000	0.0000	0.0000	0.0000
1.0(+5)	1.0000	1.0000	1.0000	1.0000	1.0000	1.0000	1.0000	1.0000	0.0000	0.0000	0.0000
5.0(+4)	1.0000	1.0000	1.0000	1.0000	1.0000	1.0000	1.0000	1.0000	0.0000	0.0000	0.0000

Table 2. (cont.)

Neutron Group Upper Energy (eV)	1.11(+6)	5.50(+5)	1.11(+5)	3.35(+3)	5.83(+2)	1.01(+2)	2.90(+1)	1.07(+1)	3.06(+0)	1.12(+0)	0.414(+0)
Production Probability	0.000000	0.000000	0.000002	0.000029	0.000093	0.000219	0.000402	0.000695	0.001232	0.002024	0.021343
Gamma Group Upper Energy (eV)	Cumulative Probability										
10.0(+6)	0.0000	0.0000	0.0338	0.0338	0.0338	0.0338	0.0338	0.0338	0.0338	0.0338	0.0338
8.0(+6)	0.0000	0.0000	0.0871	0.0871	0.0871	0.0871	0.0871	0.0871	0.0871	0.0871	0.0871
6.5(+6)	0.0000	0.0000	0.7155	0.7155	0.7155	0.7155	0.7155	0.7155	0.7155	0.7155	0.7155
5.0(+6)	0.0000	0.0000	0.8103	0.8103	0.8103	0.8103	0.8103	0.8103	0.8103	0.8103	0.8103
4.0(+6)	0.0000	0.0000	1.0000	1.0000	1.0000	1.0000	1.0000	1.0000	1.0000	1.0000	1.0000
3.0(+6)	0.0000	0.0000	1.0000	1.0000	1.0000	1.0000	1.0000	1.0000	1.0000	1.0000	1.0000
2.5(+6)	0.0000	0.0000	1.0000	1.0000	1.0000	1.0000	1.0000	1.0000	1.0000	1.0000	1.0000
2.0(+6)	0.0000	0.0000	1.0000	1.0000	1.0000	1.0000	1.0000	1.0000	1.0000	1.0000	1.0000
1.66(+6)	0.0000	0.0000	1.0000	1.0000	1.0000	1.0000	1.0000	1.0000	1.0000	1.0000	1.0000
1.33(+6)	0.0000	0.0000	1.0000	1.0000	1.0000	1.0000	1.0000	1.0000	1.0000	1.0000	1.0000
1.0(+6)	0.0000	0.0000	1.0000	1.0000	1.0000	1.0000	1.0000	1.0000	1.0000	1.0000	1.0000
8.0(+5)	0.0000	0.0000	1.0000	1.0000	1.0000	1.0000	1.0000	1.0000	1.0000	1.0000	1.0000
6.0(+5)	0.0000	0.0000	1.0000	1.0000	1.0000	1.0000	1.0000	1.0000	1.0000	1.0000	1.0000
4.0(+5)	0.0000	0.0000	1.0000	1.0000	1.0000	1.0000	1.0000	1.0000	1.0000	1.0000	1.0000
3.0(+5)	0.0000	0.0000	1.0000	1.0000	1.0000	1.0000	1.0000	1.0000	1.0000	1.0000	1.0000
2.0(+5)	0.0000	0.0000	1.0000	1.0000	1.0000	1.0000	1.0000	1.0000	1.0000	1.0000	1.0000
1.0(+5)	0.0000	0.0000	1.0000	1.0000	1.0000	1.0000	1.0000	1.0000	1.0000	1.0000	1.0000
5.0(+4)	0.0000	0.0000	1.0000	1.0000	1.0000	1.0000	1.0000	1.0000	1.0000	1.0000	1.0000

*Read as 15.0×10^6.

Table 3. Gamma-Production Probabilities for Ground

Neutron Group Upper Energy (eV)	15.0(+6)*	12.2(+6)	10.0(+6)	8.18(+6)	6.36(+6)	4.96(+6)	4.06(+6)	3.01(+6)	2.46(+6)	2.35(+6)	1.83(+6)
Production Probability	0.5900	0.5277	0.4634	0.4312	0.1476	0.1017	0.0586	0.0675	0.0523	0.0330	0.0127
Gamma Group Upper Energy (eV)	Cumulative Probability										
10.0(+6)	0.0063	0.0040	0.0005	0.0000	0.0000	0.0000	0.0000	0.0000	0.0001	0.0001	0.0002
8.0(+6)	0.1377	0.1205	0.0708	0.0103	0.0041	0.0024	0.0011	0.0005	0.0007	0.0007	0.0016
6.5(+6)	0.4079	0.4239	0.4120	0.1872	0.0124	0.0036	0.0019	0.0011	0.0018	0.0018	0.0043
5.0(+6)	0.4601	0.4666	0.4489	0.2133	0.0337	0.0111	0.0058	0.0032	0.0055	0.0057	0.0138
4.0(+6)	0.5593	0.5652	0.5758	0.5801	0.0745	0.0361	0.0175	0.0050	0.0085	0.0087	0.0213
3.0(+6)	0.6408	0.6309	0.6177	0.6167	0.1378	0.0872	0.0478	0.0054	0.0090	0.0092	0.0222
2.5(+6)	0.6805	0.6745	0.6622	0.6658	0.2905	0.2801	0.2529	0.1083	0.0200	0.0202	0.0270
2.0(+6)	0.8042	0.8126	0.8070	0.8179	0.6141	0.5904	0.5743	0.5456	0.4645	0.4646	0.2062
1.66(+6)	0.9015	0.8885	0.8838	0.9043	0.8102	0.7920	0.7910	0.8246	0.7596	0.7584	0.4348
1.33(+6)	0.9291	0.9184	0.9177	0.9388	0.8934	0.8935	0.9057	0.9327	0.9027	0.8990	0.7086
1.0(+6)	0.9438	0.9361	0.9364	0.9556	0.9279	0.9314	0.9412	0.9586	0.9401	0.9379	0.8219
8.0(+5)	0.9609	0.9555	0.9566	0.9732	0.9633	0.9698	0.9769	0.9846	0.9778	0.9771	0.9356
6.0(+5)	0.9756	0.9721	0.9734	0.9856	0.9848	0.9912	0.9958	0.9981	0.9973	0.9973	0.9940
4.0(+5)	0.9815	0.9789	0.9799	0.9891	0.9885	0.9933	0.9969	0.9986	0.9979	0.9980	0.9954
3.0(+5)	0.9878	0.9861	0.9867	0.9928	0.9924	0.9956	0.9979	0.9990	0.9986	0.9986	0.9969
2.0(+5)	0.9945	0.9937	0.9940	0.9967	0.9966	0.9980	0.9991	0.9996	0.9994	0.9994	0.9986
1.0(+5)	0.9979	0.9976	0.9977	0.9988	0.9987	0.9992	0.9996	0.9998	0.9998	0.9998	0.9995
5.0(+4)	1.0000	1.0000	1.0000	1.0000	1.0000	1.0000	1.0000	1.0000	1.0000	1.0000	1.0000

Table 3 (cont.)

Neutron Group Upper Energy (eV)	1.11(+6)	5.50(+5)	1.11(+5)	3.35(+3)	5.83(+2)	1.01(+2)	2.90(+1)	1.07(+1)	3.06(+0)	1.12(+0)	0.414(+0)
Production Probability	0.0009	0.0012	0.0020	0.0034	0.0034	0.0038	0.0042	0.0050	0.0065	0.0085	0.0431
Gamma Group Upper Energy (eV)	Cumulative Probability										
10.0(+6)	0.0035	0.0046	0.0045	0.0052	0.0052	0.0048	0.0042	0.0035	0.0027	0.0020	0.0023
8.0(+6)	0.0256	0.0382	0.0383	0.0365	0.0355	0.0354	0.0352	0.0351	0.0346	0.0344	0.0341
6.5(+6)	0.0661	0.0938	0.0933	0.0961	0.0948	0.0910	0.0862	0.0802	0.0732	0.0673	0.0695
5.0(+6)	0.2139	0.2939	0.2907	0.3149	0.3131	0.2938	0.2699	0.2386	0.2044	0.1747	0.1875
4.0(+6)	0.3315	0.4544	0.4491	0.4887	0.4862	0.4553	0.4172	0.3670	0.3124	0.2649	0.2855
3.0(+6)	0.3444	0.4774	0.4730	0.5055	0.5016	0.4735	0.4385	0.3929	0.3428	0.2993	0.3175
2.5(+6)	0.3744	0.5226	0.5185	0.5584	0.5725	0.5654	0.5597	0.5482	0.5408	0.5324	0.5417
2.0(+6)	0.4272	0.6093	0.6071	0.6302	0.6405	0.6393	0.6399	0.6380	0.6395	0.6394	0.6435
1.66(+6)	0.4597	0.6569	0.6548	0.6768	0.6860	0.6841	0.6837	0.6807	0.6807	0.6795	0.6836
1.33(+6)	0.4989	0.7159	0.7141	0.7325	0.7402	0.7385	0.7381	0.7354	0.7352	0.7340	0.7376
1.0(+6)	0.6483	0.7536	0.7522	0.7668	0.7733	0.7725	0.7729	0.7717	0.7727	0.7727	0.7752
8.0(+5)	0.8050	0.8019	0.8009	0.8116	0.8166	0.8165	0.8174	0.8173	0.8188	0.8195	0.8212
6.0(+5)	0.9063	0.8604	0.8597	0.8667	0.8702	0.8704	0.8713	0.8717	0.8733	0.8742	0.8751
4.0(+5)	0.9285	0.8935	0.8930	0.8981	0.9008	0.9010	0.9019	0.9023	0.9037	0.9045	0.9051
3.0(+5)	0.9524	0.9292	0.9289	0.9322	0.9339	0.9341	0.9348	0.9352	0.9362	0.9368	0.9372
2.0(+5)	0.9781	0.9675	0.9674	0.9688	0.9696	0.9698	0.9701	0.9703	0.9708	0.9711	0.9713
1.0(+5)	0.9917	0.9877	0.9876	0.9882	0.9885	0.9885	0.9886	0.9887	0.9889	0.9890	0.9891
5.0(+5)	1.0000	1.0000	1.0000	1.0000	1.0000	1.0000	1.0000	1.0000	1.0000	1.0000	1.0000

*Read as 15.0×10^6.

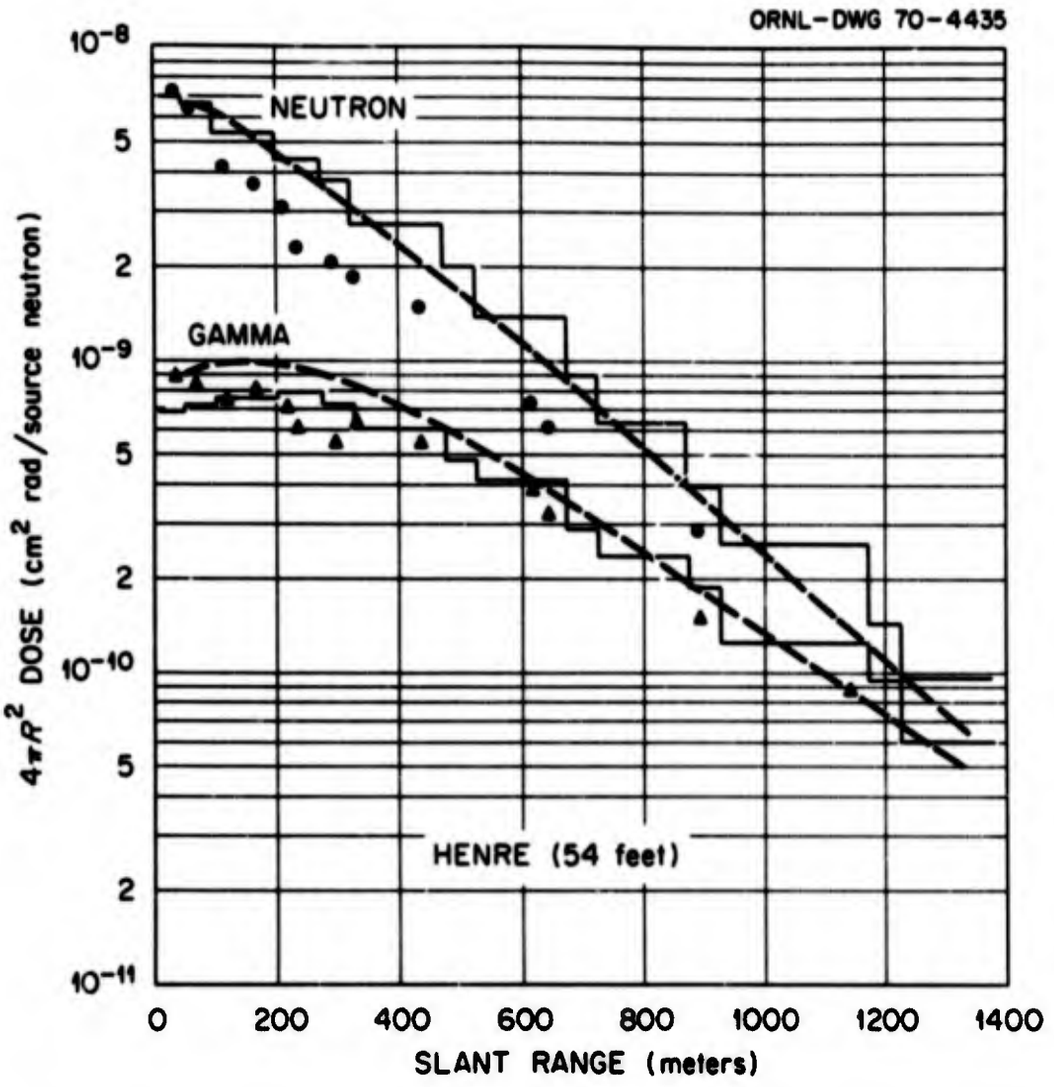

Fig. 2. Comparison of Measured and Calculated Neutron and Secondary Gamma-Ray Doses for the HENRE Accelerator Operating at 54 ft Above the Ground. Calculations are for a 50-ft, 12.2- to 15-MeV Source. —— Monte Carlo; --- Discrete Ordinates; 0,Δ ref. 21.

such as hydrogen content would have a large effect. The contribution from reactor gamma rays was included in the calculation of the secondary gamma-ray dose. The HENRE results have not been renormalized to account for anisotropy of the source. The correction factor for anisotropy is probably between 0.65 and 0.83, and the corrected experimental results would be higher;[22,28] thus, better agreement between measurements and calculations would result. This agreement for the nominal fission (Godiva leakage spectrum) and for the nominal 14-MeV sources provides reasonable confidence in the cross sections used.

An intercomparison between the Monte Carlo and discrete ordinates results was made in various degrees of detail as an additional check of the calculational techniques. That is, results of dose versus range for a 12.2- to 15-MeV neutron source (see Fig. 3) illustrate that there is good agreement for both neutrons and secondary gamma rays. The corner in the discrete ordinates curve is due to connecting the calculated values at three points by straight lines. The Monte Carlo results of secondary gamma rays include only those gamma rays produced by inelastic scattering and fast-neutron capture and therefore should be smaller than the discrete ordinates results. A more detailed comparison - that of neutron energy spectra at a slant range of 900 m - is shown in Fig. 4. The agreement is still fairly good with differences in the 10- to 15-MeV energy range primarily being due to the effect of the weighting of the multigroup cross sections. A more differential comparison, that of the angular distribution of the 12.2- to 15-MeV fluence at 300 m due to a 12.2- to 15-MeV source, is shown in Fig. 5. The disagreements are as large as a factor of 2.5 in the wings of the angular distribution near $\mu = \pm 1$, but are fairly good where the intensity is high. These results are very sensitive to the angular distribution of within-group

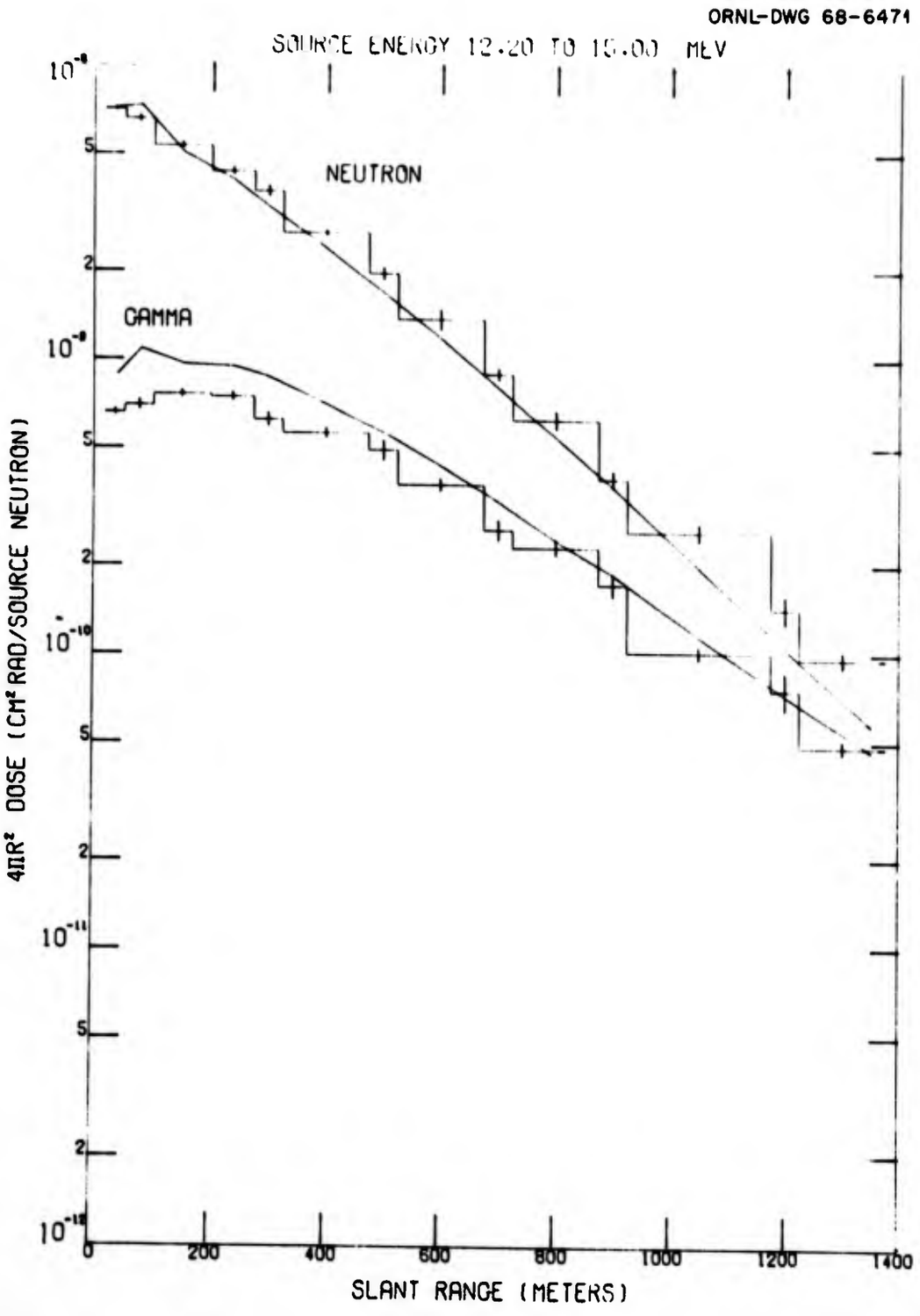

Fig. 3. Comparison of Monte Carlo and Discrete Ordinates Results for Neutron and Secondary Gamma-Ray Dose Due to a 12.2- to 15-MeV Neutron Source at an Altitude of 50 ft.

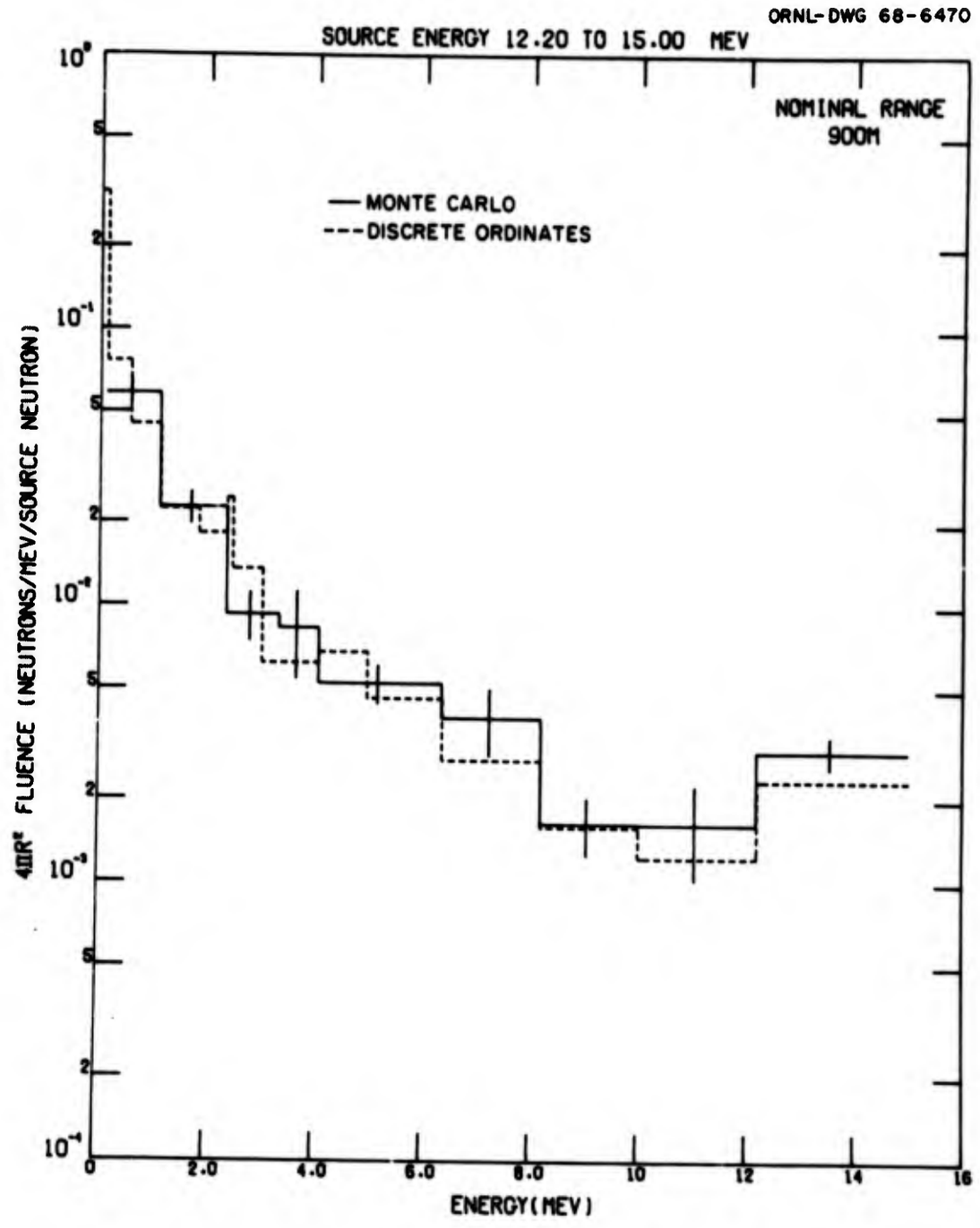

Fig. 4. Comparison of Monte Carlo and Discrete Ordinates Results for Neutron Fluence at 900 m Due to a 12.2- to 15-MeV Neutron Source at an Altitude of 50 ft.

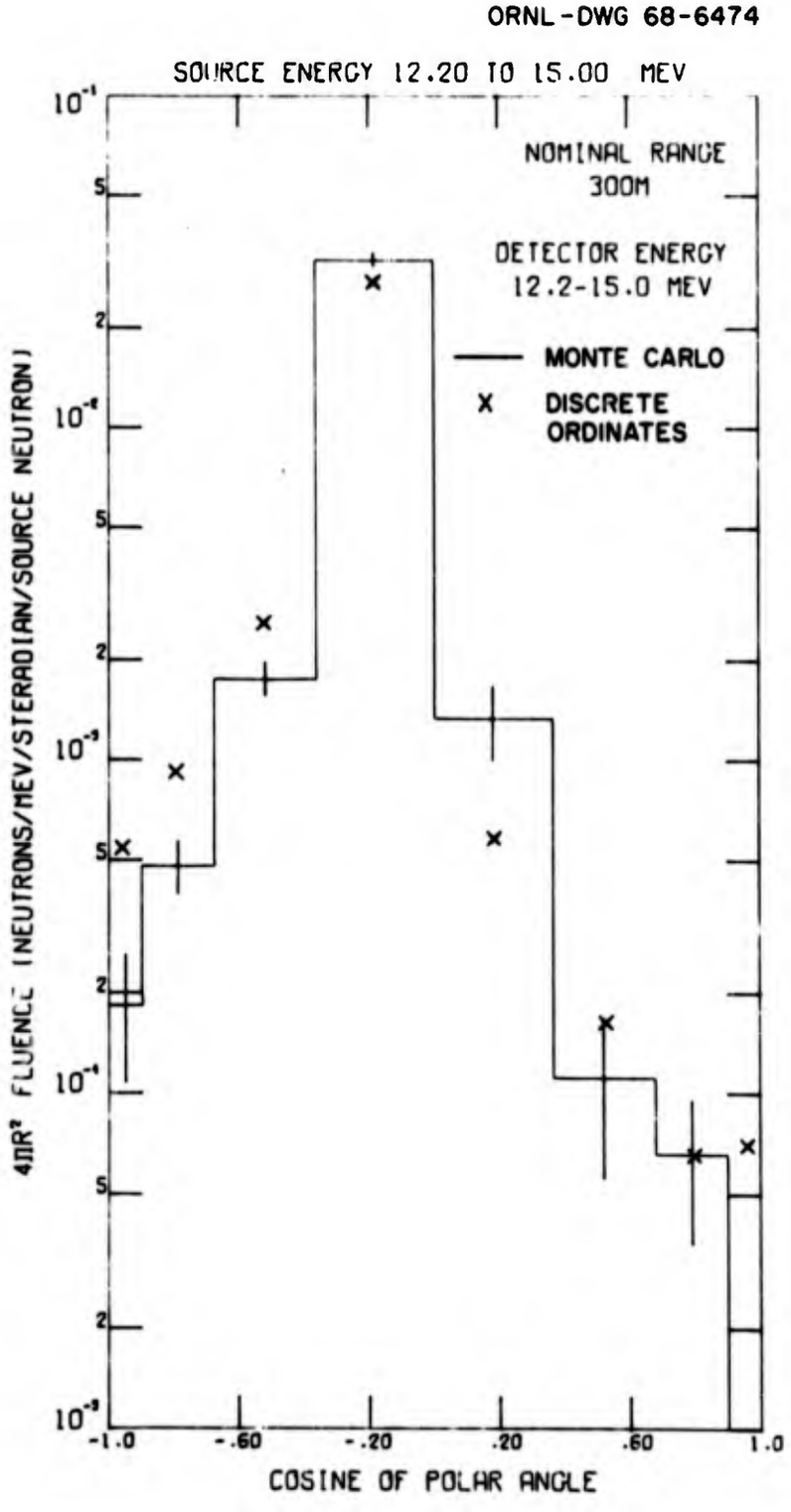

Fig. 5. Comparison of Monte Carlo and Discrete Ordinates Results for the Angular Distribution of the 12.2- to 15-MeV Neutron Fluence at a Range of 300 m Due to a 12.2- to 15-MeV Neutron Source.

scattering and illustrate the broadening effects of using P_3 cross sections in the discrete ordinates calculations when compared to the angular distribution obtained using P_8 cross sections in the Monte Carlo calculations.

The agreement of the results of the two calculational methods provides credibility for the transport techniques. This, combined with the agreement with experimental data, gives additional confidence in the validity of the results presented here.

RESULTS

Results of the calculations for a source height of 50 ft are given in ref. 23 and are available from RSIC.[24] The Monte Carlo results in ref. 23 are given for 13 ranges out to 1375 m, for 9 neutron detector energy intervals and 2 angles, 7 gamma-ray energies and 4 angles, and 10 detector-dependent time bins. The discrete ordinates results, also given in ref. 23, are for 22 neutron energies, 18 gamma-ray energies, 13 spatial intervals, and 40 angles. Besides the full differential results, various integrals over angle, time, and energy intervals are determined. The data file in RSIC includes an editing and folding code so that results for different source-energy spectra or detector responses may be obtained.

The results for infinite air are given in ref. 25 and contain data for 15 spatial intervals, 22 neutron and 18 gamma groups, and 17 angular directions. Integrals over angle and weighted sums over energy are made to provide for neutrons the angular variation of Henderson dose, Snyder-Neufeld dose, tissue kerma, midphantom dose, concrete kerma, air kerma, ionizing silicon kerma, and nonionizing kerma. For gamma rays, results are given for Henderson dose, concrete kerma, air kerma, and silicon kerma.

EFFECT OF THE GROUND ON STEADY-STATE RESULTS

The results presented in this section are examples of some of the calculations and illustrate the effects of the source and detector height variations. In particular, to determine the effect of the air-ground interface, three source geometries are considered: (1) a source located at 50 ft above the ground, (2) a source at 1125 ft, and (3) infinite homogeneous air. Detector positions varied from the ground level to a height of 1200 ft. The results for the 50-ft source height and a detector on the ground and the results for infinite air provide the limiting cases of a surface burst with the detector on the ground and the case of a source and receiver high in the air. Results for both fission and 12.2- to 15-MeV sources are presented since these tend to be the extremes in the effect of source energy spectra on the results of interest. The effects of the ground on the neutron and gamma-ray dose are shown, and then the effects on more differential qualities, such as energy spectra and angular distributions, are discussed.

Figure 6 shows the variation with ranges of the $4\pi R^2$ Henderson dose in infinite air for fission and 12.2- to 15-MeV sources. Even at a range of 2500 m the exponential attenuation of the neutron dose curves for the fission source and for the 14-MeV source have not reached the same slope. (After about 3000 m they tend to be parallel.) The secondary gamma-ray dose for a 12.2- to 15-MeV source is a factor of 10 greater than that for a fission source. Thus, if there is approximately 10% of a 12.2- to 15-MeV source in a mixed spectrum, the secondary gamma-ray dose will be equally divided between components from the fission and the 12.2- to 15-MeV source.

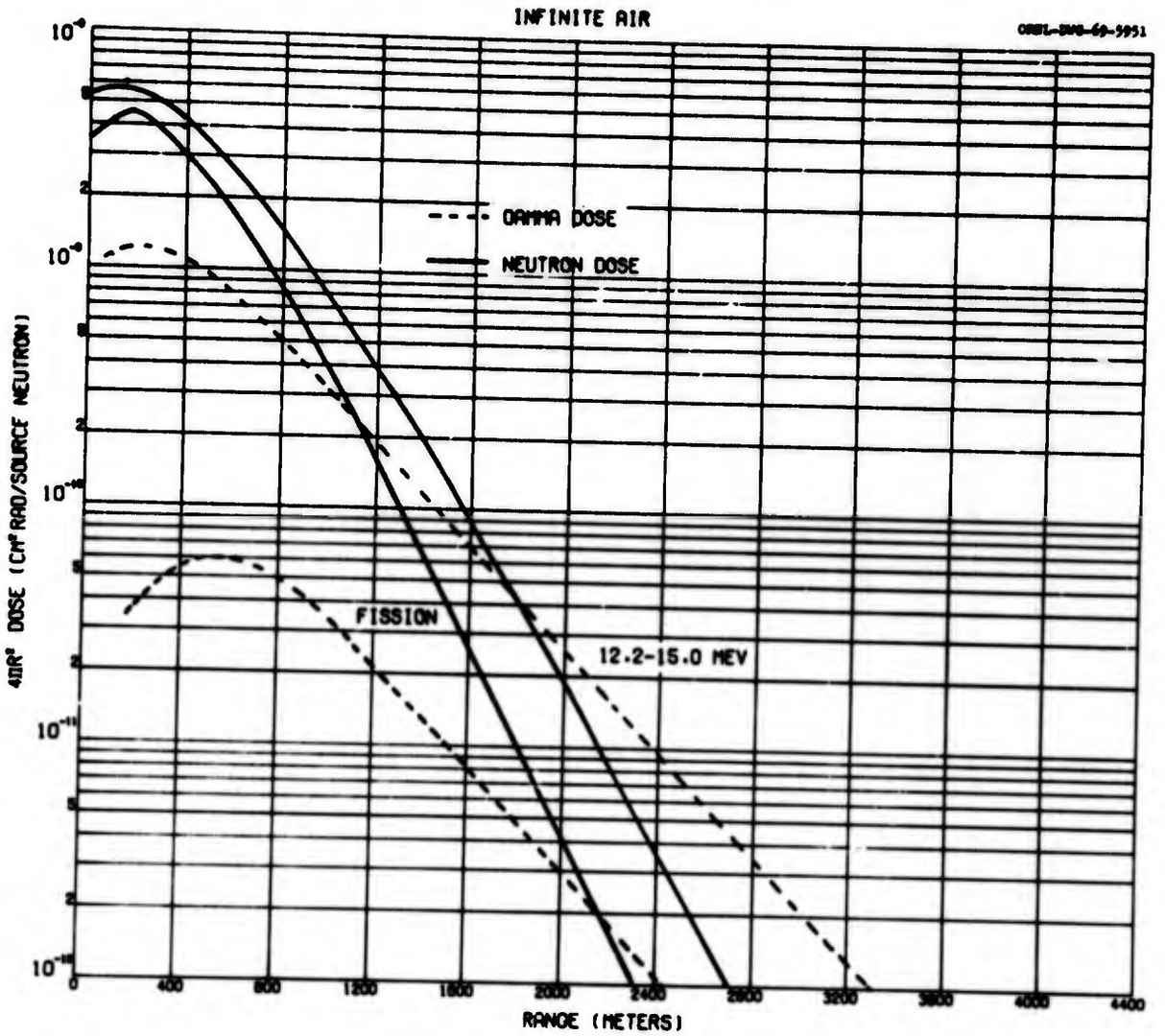

Fig. 6. Neutron and Secondary Gamma-Ray Dose in Infinite Air Due to Fission and 12.2- to 15-MeV Neutron Sources.

Because most of the following discussion involves comparisons of dose, it is necessary to know whether results for other response functions vary in the same way.

Figure 7 shows a comparison between tissue dose and other types of responses versus range for a 12.2- to 15-MeV source in infinite air. The shapes of the curves for ranges less than 600 m are different; however, they become almost parallel for larger ranges. Thus these different responses are not significantly different in shape but are different only in magnitude. The conclusions regarding the effect of source and detector height on dose curves are as a first approximation also true for other responses.

Figures 8 through 10 illustrate the effect of the ground on the neutron and gamma-ray dose as the source height or detector height is varied. Figure 8 shows the effect of varying the height of a 12.2- to 15-MeV source for a detector 1 m above the ground. The infinite air results are shown for comparison. For the neutron dose the effect of changing from a source height of 15 to 343 m is essentially the same as that predicted by French.[26] The results for the 343-m source height show a different relaxation length from the infinite air result. The prediction scheme of French would give the same relaxation length for all source heights. Thus these calculations show that at short ranges the ground acts as a reflector, but at large ranges the ground behaves as an absorber. This behavior is similar to that reported previously.[18] The shorter relaxation length for a source height of 343 m for infinite air is due primarily to the detector being near the ground. The same conclusions hold for the secondary gamma-ray dose curves shown in Fig. 8. For a fission source, Fig. 9, the relaxation length

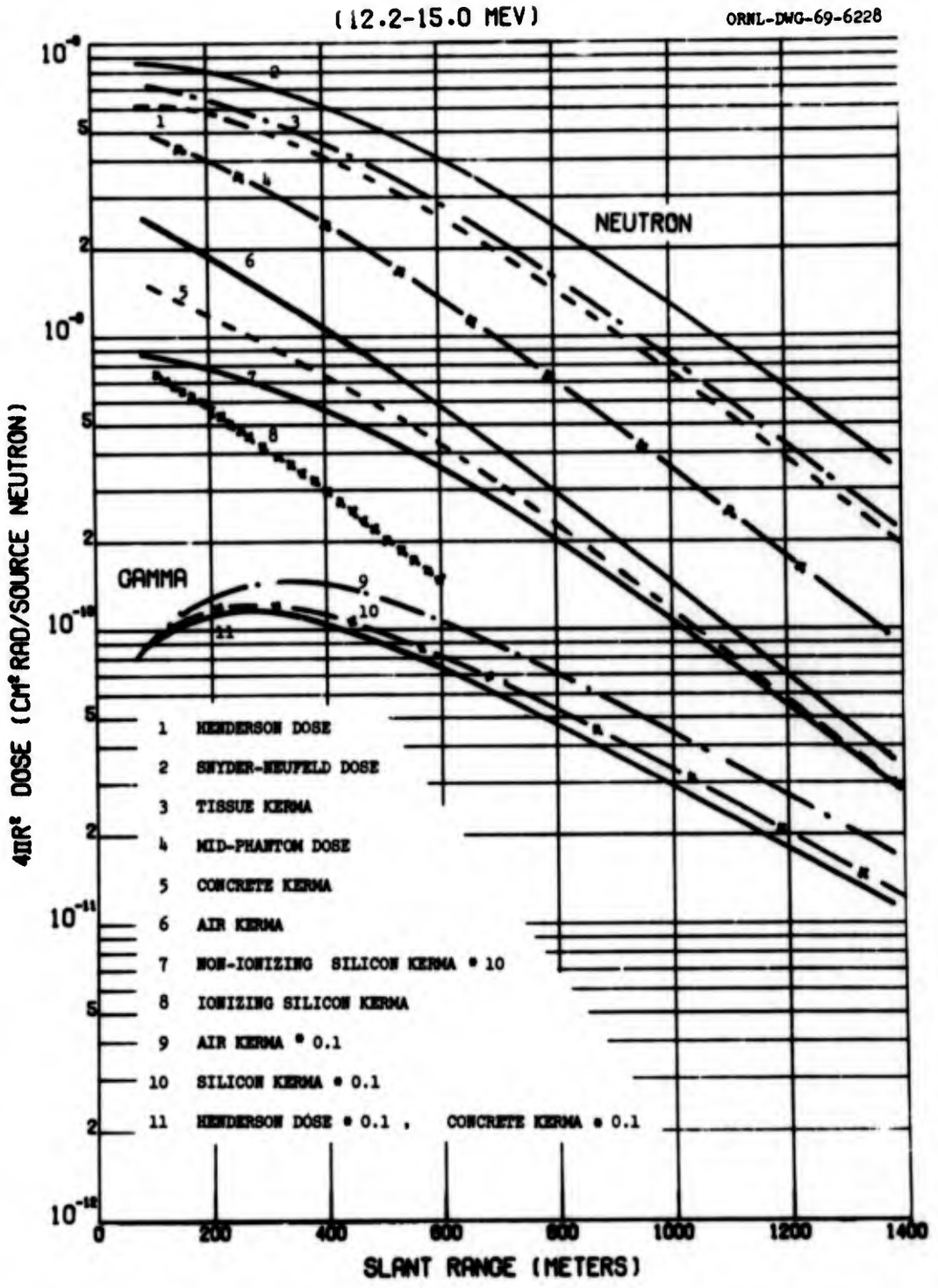

Fig. 7. Comparison of the Spatial Behavior of Different Responses for a 12.2- to 15-MeV Neutron Source in Infinite Air.

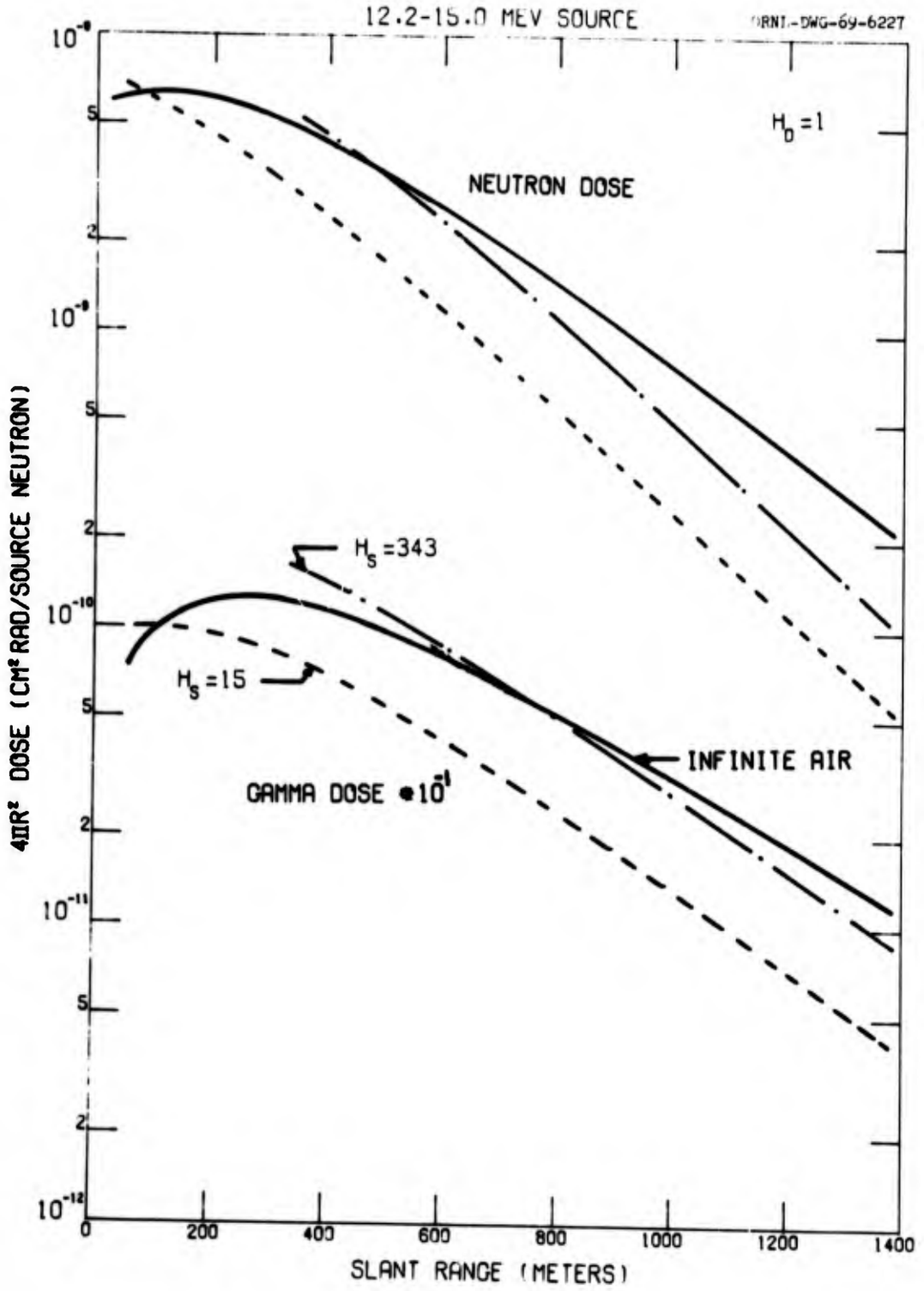

Fig. 8. Variation of Neutron and Secondary Gamma-Ray Dose as a Function of Source Height for a Detector 1 m Above the Ground - 12.2- to 15-MeV Source.

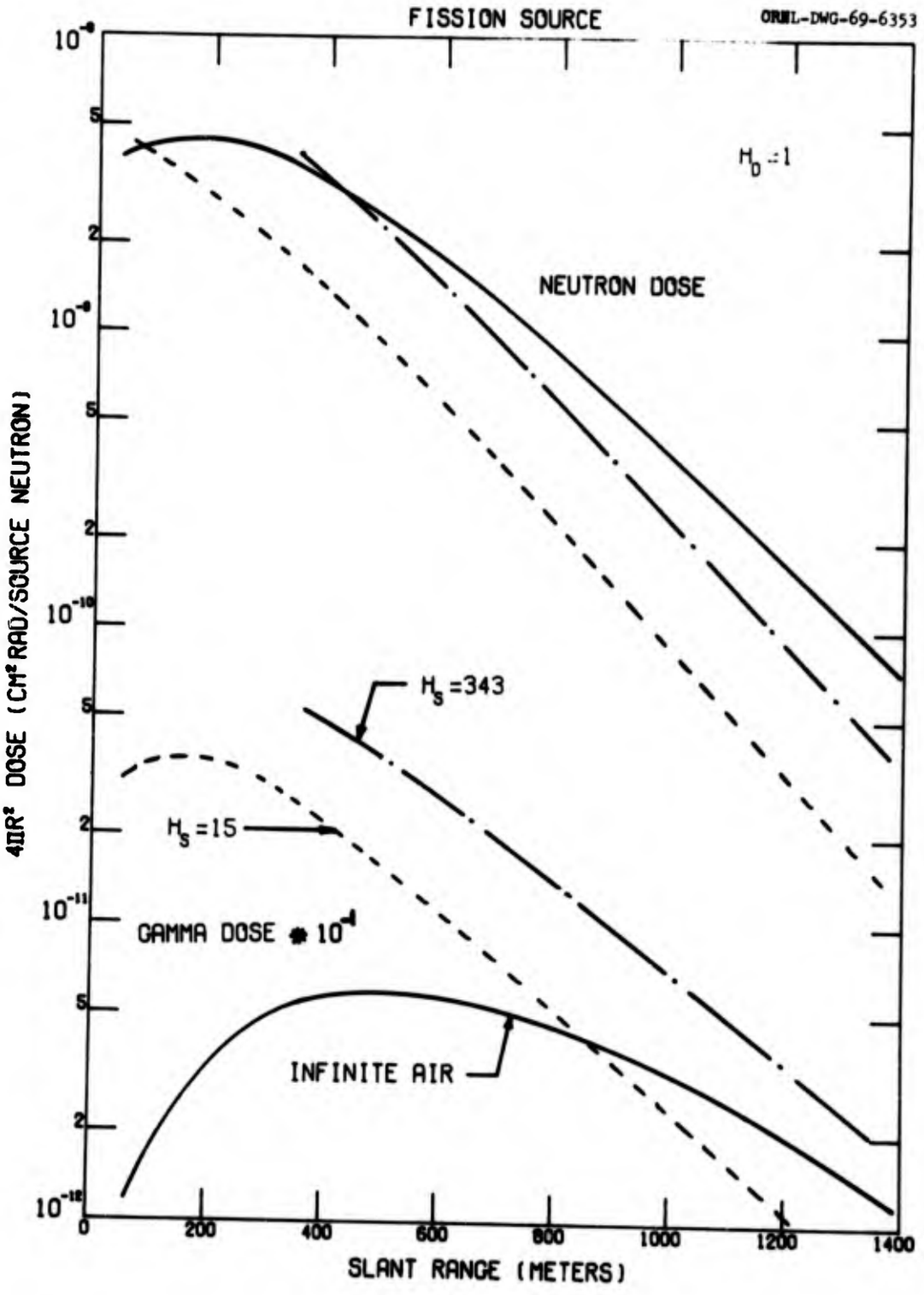

Fig. 9. Variation of Neutron and Secondary Gamma-Ray Dose as a Function of Source Height for a Detector 1 m Above the Ground - Fission Source.

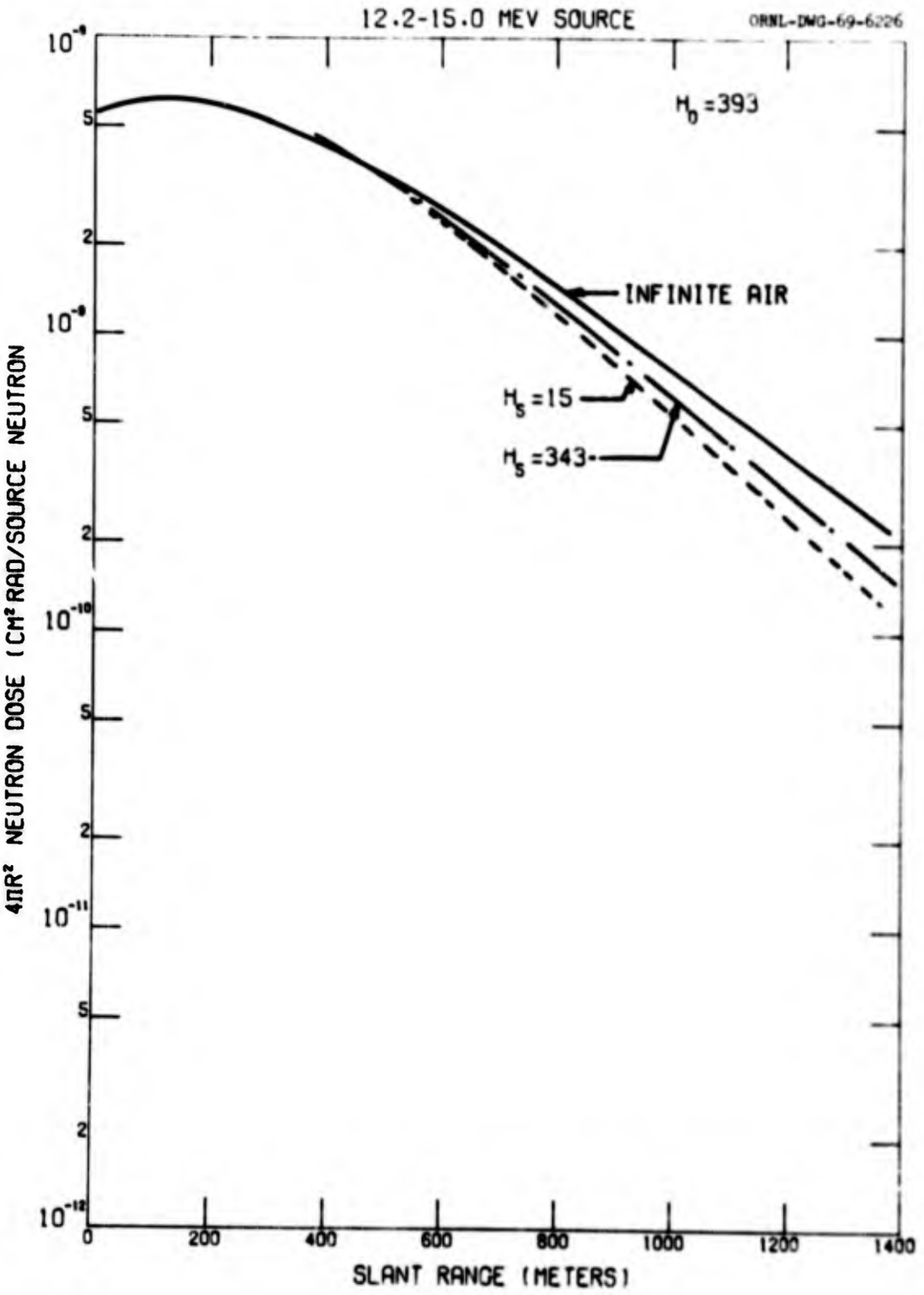

Fig. 10. Variation of Neutron Dose as a Function of Source Height for a Detector 393 m Above the Ground - 12.2- to 15-MeV Source.

for the neutron dose also varies with altitude, and the results are similar to the 12.2- to 15-MeV case. However, for the secondary gamma-ray dose a completely different behavior is noted. That is, the ground enhances the secondary gamma-ray dose even for source heights of 343 m. This is due primarily to thermal capture in the ground. As the slant range increases results for infinite air and for the 343-m source height approach each other as the importance of thermal capture in the ground decreases.

When the detector is at a height of 393 m, the effect of source height is less pronounced (Fig. 10). The effect of the source height for this case has the same trend and approximate magnitude as that predicted by French;[23] however, two things not included in the prediction scheme of French should be noted: (1) all three curves have different relaxation lengths, and (2) for a source at 343 m and a detector at 393 m the curves still lie below those for infinite air. For these source and detector heights the prediction scheme of French would give the same relaxation length as infinite air.

In many situations one is interested in a detailed description of the radiation field at the air-ground interface. As noted before, the effect of the ground on the radiation field is a function of range, and the entire set of results is a very large array of numbers. Therefore, only representative results will be given here. A more complete presentation of the results is given in refs. 23 and 25. The neutron energy spectra at a slant range of 900 m for a 50-ft source height (dashed line) and for infinite air (hashed lines) are shown in Fig. 11. The solid line is a Monte Carlo calculation for a source height of 50 ft. The energy spectra essentially agree in shape but are different in magnitude by about the same factor as that

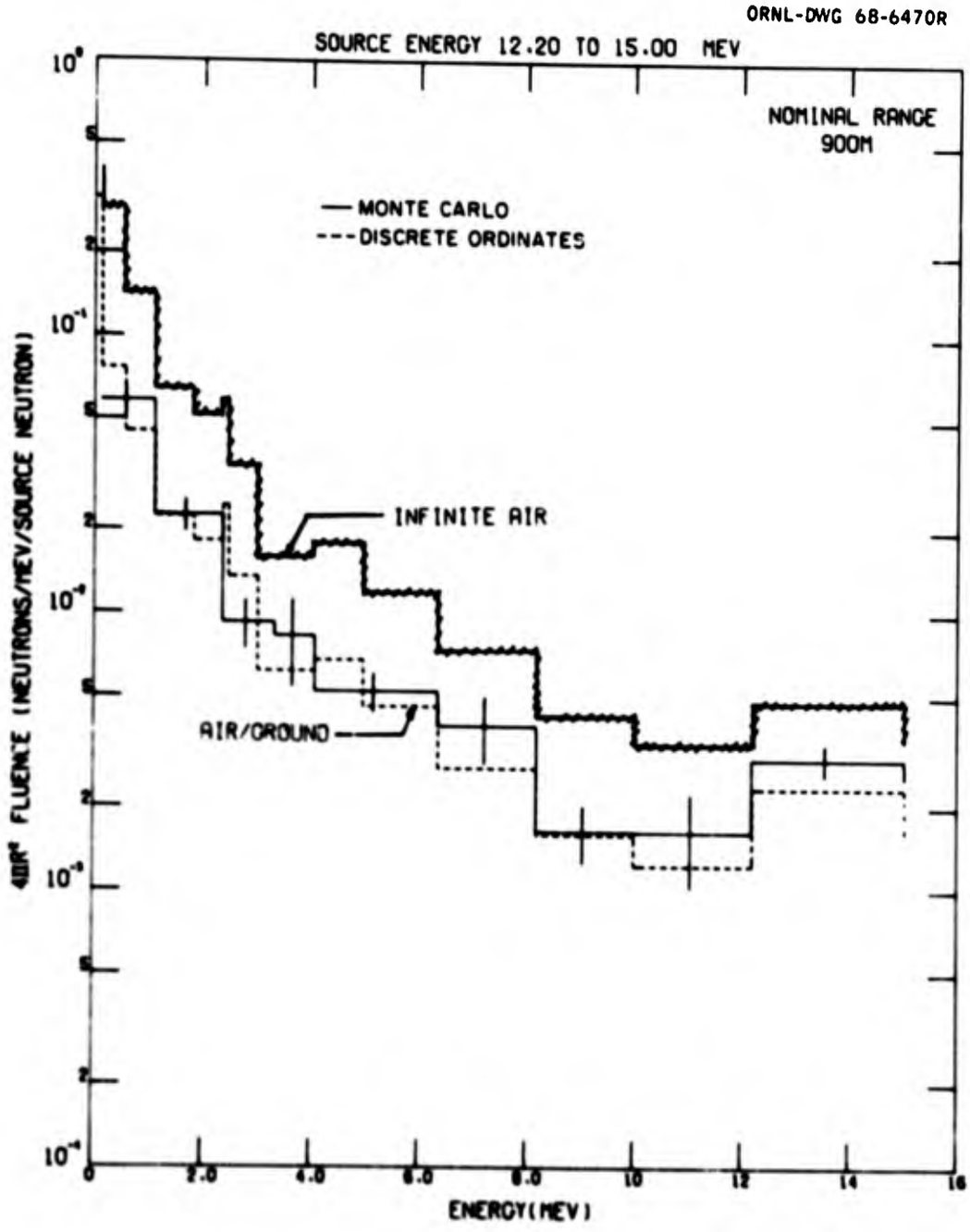

Fig. 11. Energy Distribution of the Fast-Neutron Fluence at a Slant Range of 900 m Due to a 12.2- to 15-MeV Source. /// Infinite Air; --- Discrete Ordinates Results for Source Height of 50 ft; —+— Monte Carlo Results for a Source Height of 50 ft.

between the dose curves at the 900-m range (Fig. 8). That is, the correction at this range that would be predicted by the procedure of French would be adequate for the fast-neutron spectra.

For a fission source the results are slightly different (see Fig. 12). The presence of the ground reduces the <2-MeV component by about the same amount as it reduces the dose (see Fig. 9); however, the high-energy component is not reduced as much. A constant reduction factor for all energies would not be a very bad assumption, however.

In calculations of the transmission of radiation through slits and entranceways, the angular distribution at the air-ground interface is needed. Figure 13 shows the angular variation of the neutron dose at 900 m for a 12.2- to 15-MeV source. The angle is measured from the source receiver axis; thus, a cosine of +1 is along the direction from source to receiver. For the air-ground results the dose is plotted as a function of polar angle in the azimuthal angle interval nearest the plane perpendicular to the ground along the source detector axis. Of course, the dose is not azimuthally symmetric and the polar variation would be different for other azimuthal angles. Note that the ground does change the magnitude of the dose as noted before, but the shape is essentially the same as that for infinite air. Essentially the same effects were observed for a fission source.

In summarizing the effect of the ground on the steady-state neutron field, the fast-neutron energy spectra and angular distribution can, as a reasonable first approximation, be taken from infinite air results with a modification in intensity only.

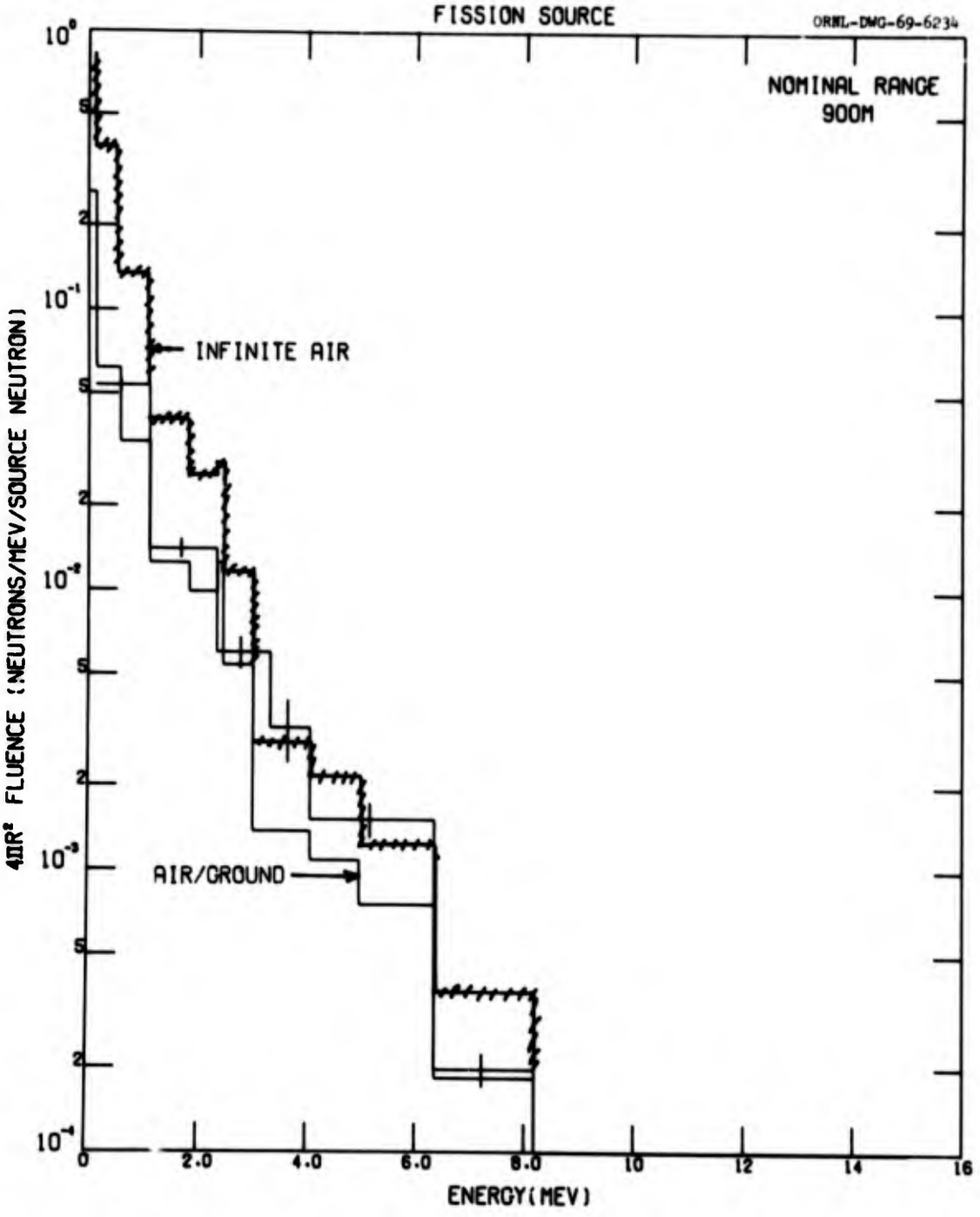

Fig. 12. Energy Distribution of the Fast Neutrons at a Slant Range of 900 m Due to a Fission Source. /// Infinite Air; --- Discrete Ordinates Results for a Source Height of 50 ft; —|— Monte Carlo Results for a Source Height of 50 ft.

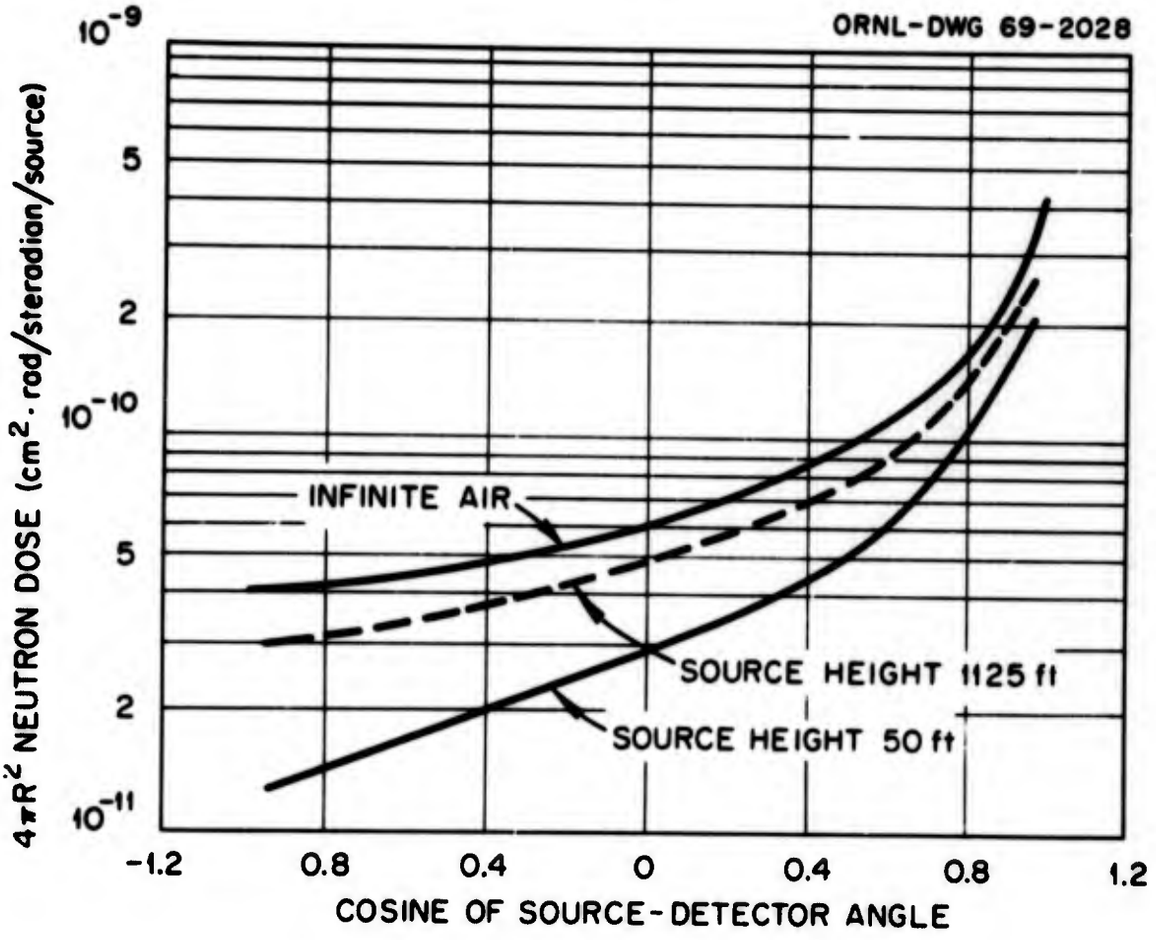

Fig. 13. Angular Distribution of Henderson Neutron Dose for a Detector 1 m Above the Ground at a Slant Range of 900 m as a Function of Source Height.

For secondary gamma rays the problem is more complex. The effect of the ground on the gamma-ray energy spectrum at a range of 900 m for a 12.2- to 15-MeV source is shown in Fig. 14. Again, the shape of the spectra for infinite air and air/ground is essentially the same with an intensity variation proportional to the dose (see Fig. 8). For a fission source (Fig. 15) the effect of the ground is much larger. Figure 9 shows that the dose is essentially the same at this range, whereas Fig. 15 shows that the spectrum is different. There is a higher component from nitrogen capture and a lower component (below 3 MeV) due to inelastic scattering and neutron capture in the ground.

The angular distribution of the secondary gamma-ray dose at 900 m due to a 12.2- to 15-MeV source is shown in Fig. 16. As before, the air-ground results are plotted as a function of the polar angle from the source receiver axis. The effect of the ground is most pronounced for a 50-ft source height, indicating an angular distribution that is perhaps 30% more peaked in the forward direction. The angular distribution for gamma-ray dose due to a fission source is essentially the same as that for the 12.2- to 15-MeV source.

EFFECT OF THE GROUND ON TIME-DEPENDENT RESULTS

Effects of the ground on time-dependent quantities are pronounced in some time intervals but are very small for other intervals. The short-time dose rate for both 12.2- to 15-MeV and fission sources at a slant range of 900 m due to a source at 50 ft is shown in Fig. 17. The dose rates for a fission source are much more spread out in time due to the spread in the source energies. Results for different source-energy groups and ranges are given in ref. 23. If the time scale is normalized

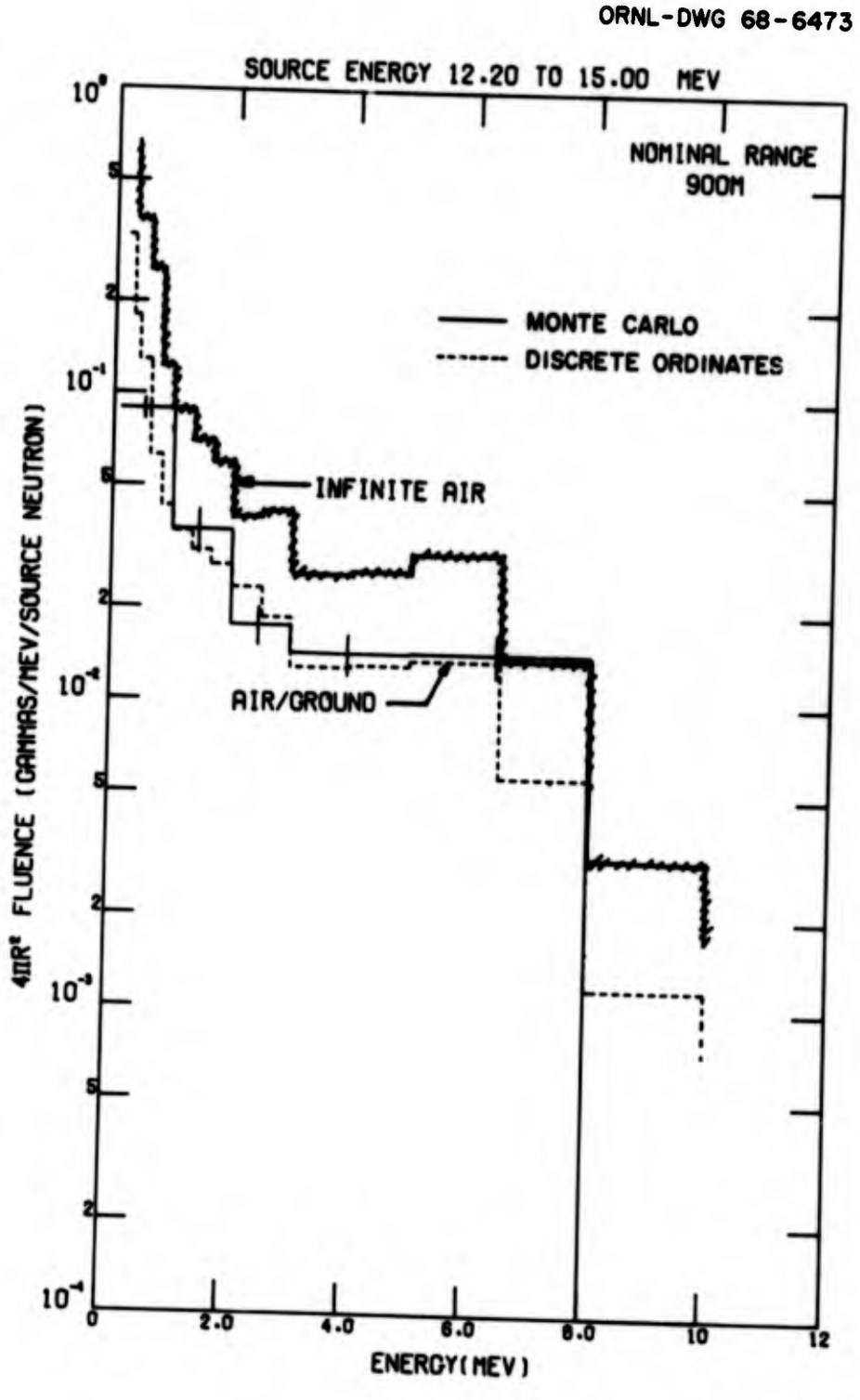

Fig. 14. Secondary Gamma-Ray Energy Spectra at a Slant Range of 900 m Due to a 12.2- to 15-MeV Neutron Source. /// Infinite Air; --- Discrete Ordinates Results for a Source at 50 ft; —+— Monte Carlo Results for a Source at 50 ft.

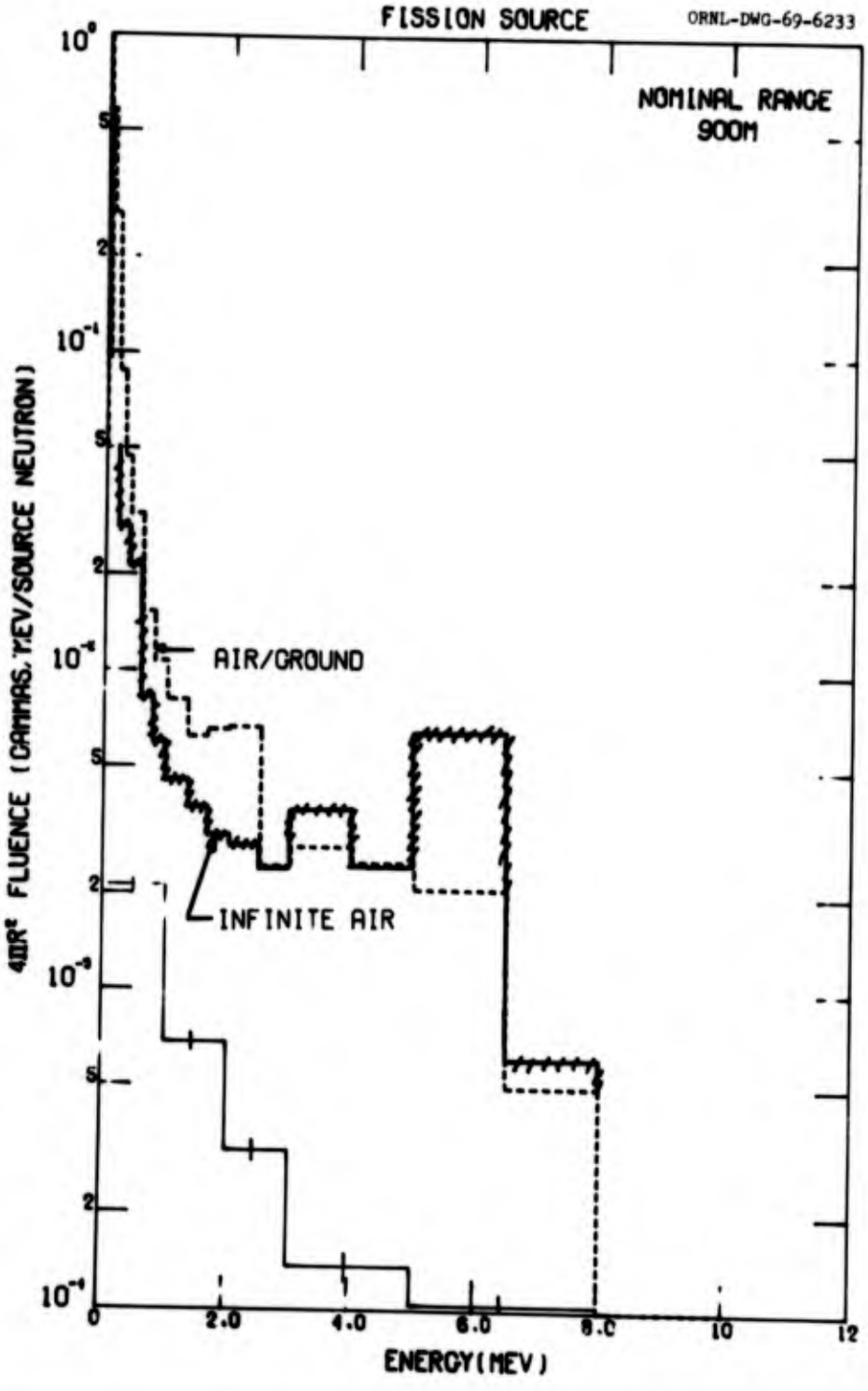

Fig. 15. Secondary Gamma-Ray Energy Spectra at a Slant Range of 900 m Due to a Fission Source. /// Infinite Air; --- Discrete Ordinates Results for Source Height of 50 ft; —|— Monte Carlo Results for Fast-Neutron-Induced Gamma Rays Due to a Source at 50 ft.

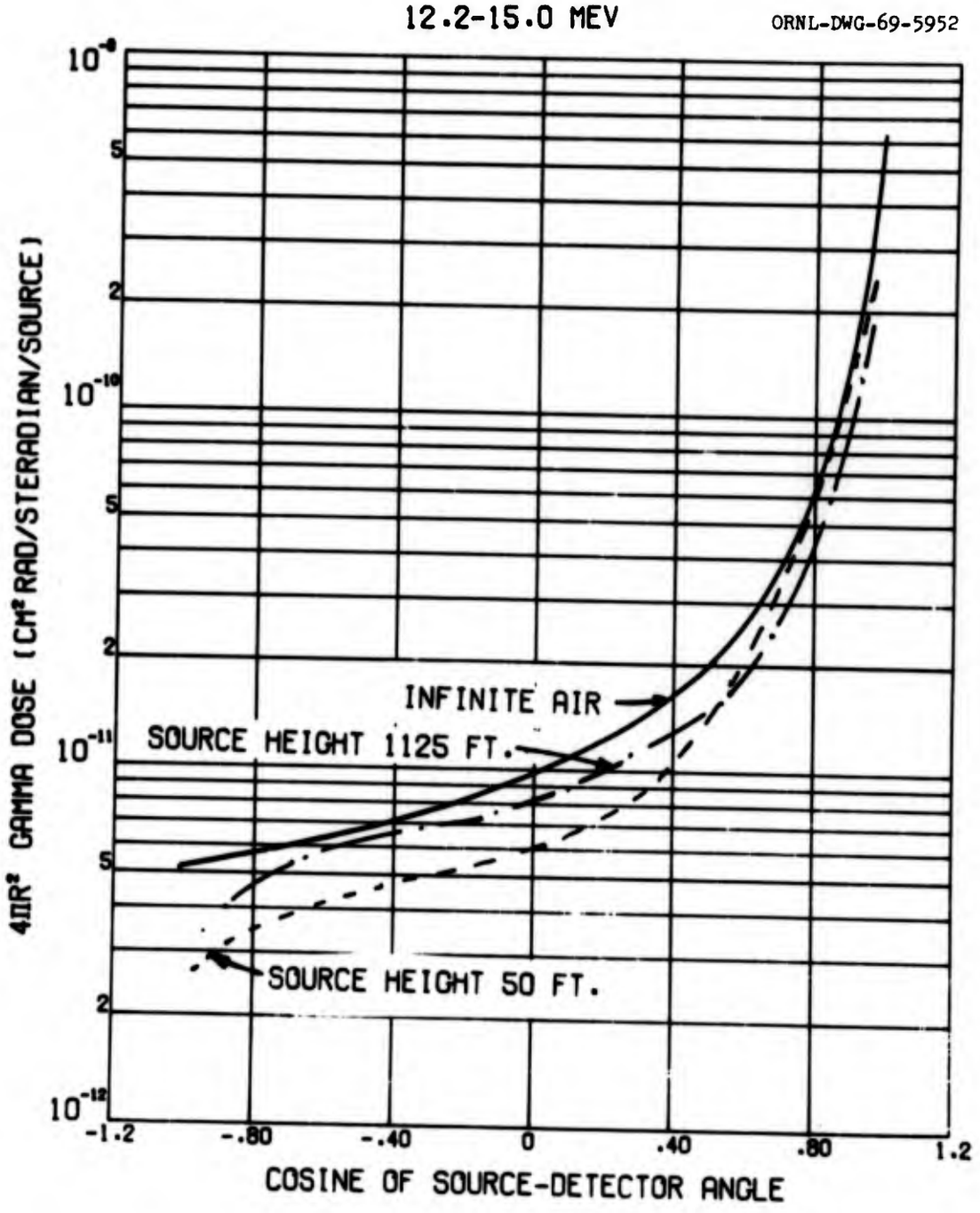

Fig. 16. Angular Distribution of Secondary Gamma-Ray Dose at 900 m Due to a 12.2- to 15-MeV Neutron Source at Various Heights.

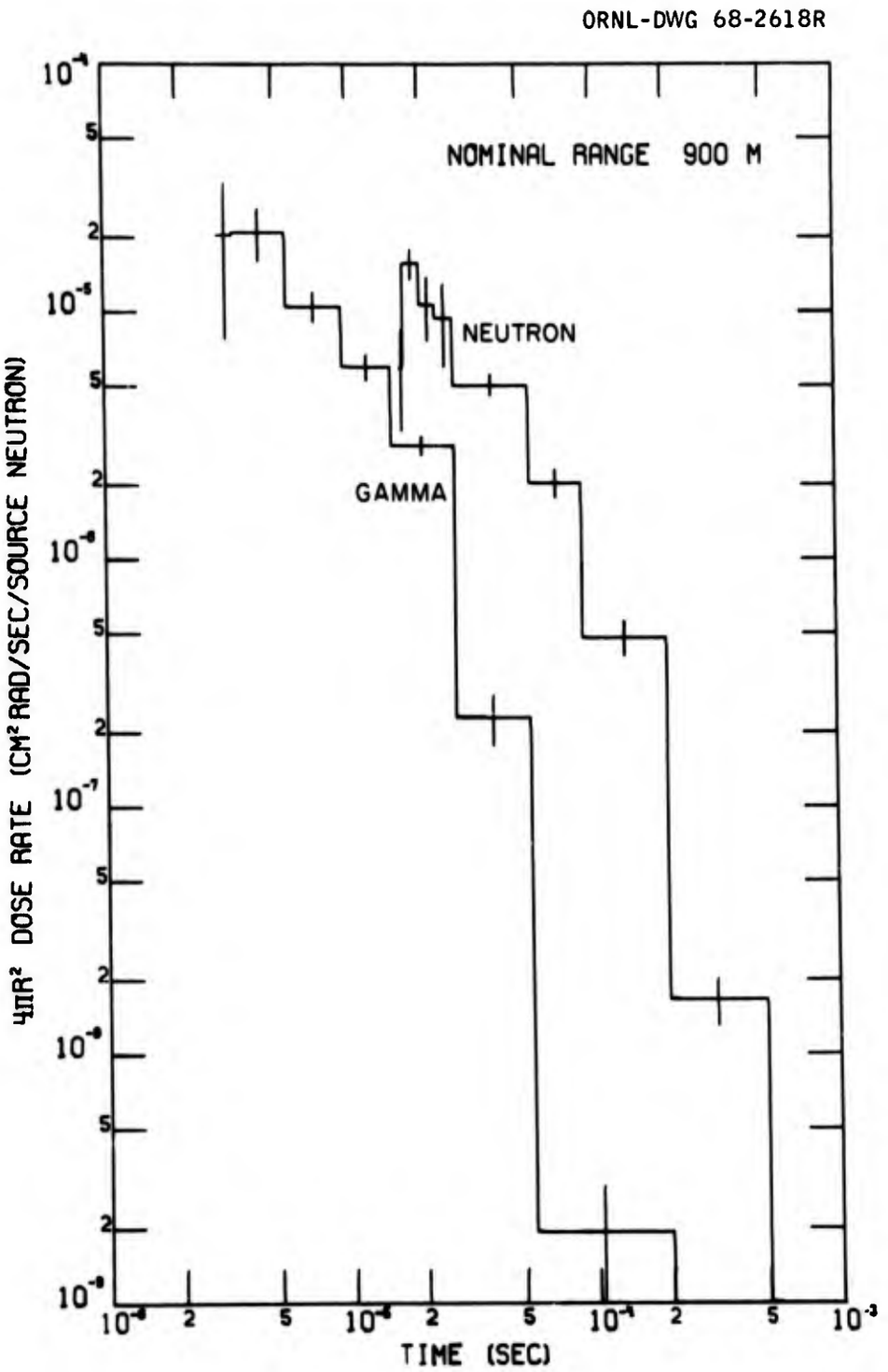

Fig. 17. Short-Time Neutron and Secondary Gamma-Ray Dose Rates Due to Fission and 12.2- to 15-MeV Neutron Sources.

by the minimum time of arrival of radiation at the detector and the dose is normalized to unity, then both neutron and secondary gamma-ray dose-rate distributions are similar (see Fig. 18). Results are given for 150, 300, 600, 900, and 1200 m for both neutron and gamma-ray dose rates; the dashed curves are gamma-ray dose rates. It is difficult to distinguish between these curves which clearly illustrates a conclusion that the short-time neutron and gamma-ray dose rates may be obtained to a first approximation ($\pm$ factor of 3) from a single curve fit to these results. The source energy spectra are important factors in determining the time-dependent dose rate as indicated by the difference in shape of the two figures.

The full time-dependent secondary gamma-ray dose rate due to an instantaneous 12.2- to 15-MeV source at a range of 300 m in infinite air is shown in Fig. 19. The solid histogram shows Monte Carlo results; the circles are time-dependent discrete ordinates results.[27] The dashed-line histogram is the gamma-ray dose curve for a source height of 50 ft above the air-ground interface. Several things should be noted. The gamma-ray dose rate is essentially constant until the neutron wave front reaches the detector ($\sim$5.6 μsec at this range) and then falls rapidly for several decades. In infinite air the dose rate drops six orders of magnitude by the time neutrons are thermalized in air (10^{4} sec). For the air-ground case the moderation in the ground is much faster (the ground contains approximately 7% water), and thus the gamma-ray dose rate falls less rapidly, since thermal-capture gamma rays are present at relatively short times. For this source energy the area under the thermal-capture part of the infinite air curve is approximately 7% of the total. The gap in the Monte Carlo results for infinite air in the time interval from 10^{-4} to 10^{-3} is due to the importance

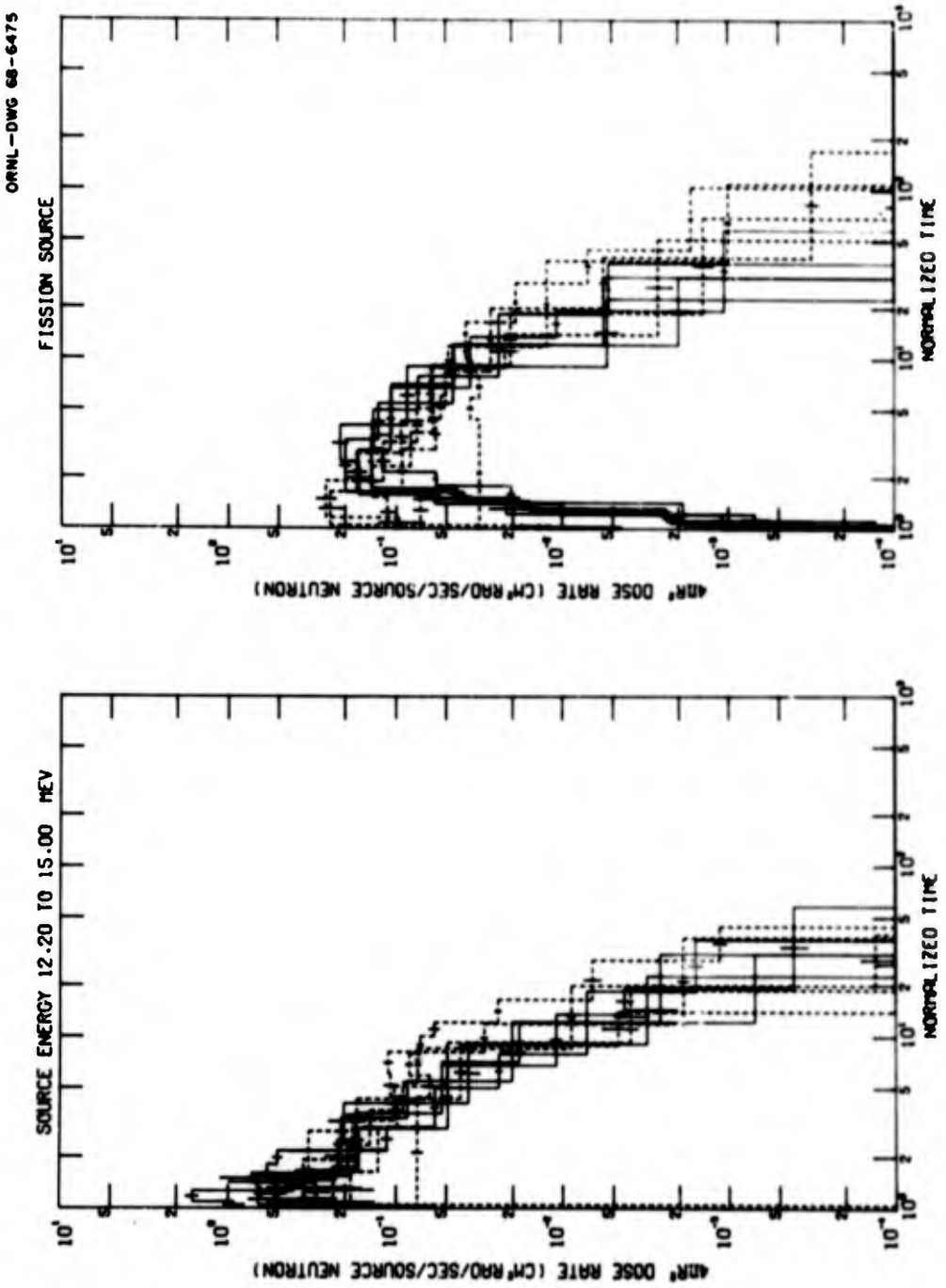

Fig. 18. Normalized Time Dependence of Neutron and Gamma-Ray Dose Rates for Detectors at 150, 300, 600, 900, and 1200 m from 12.2- to 15-MeV and Fission Sources.

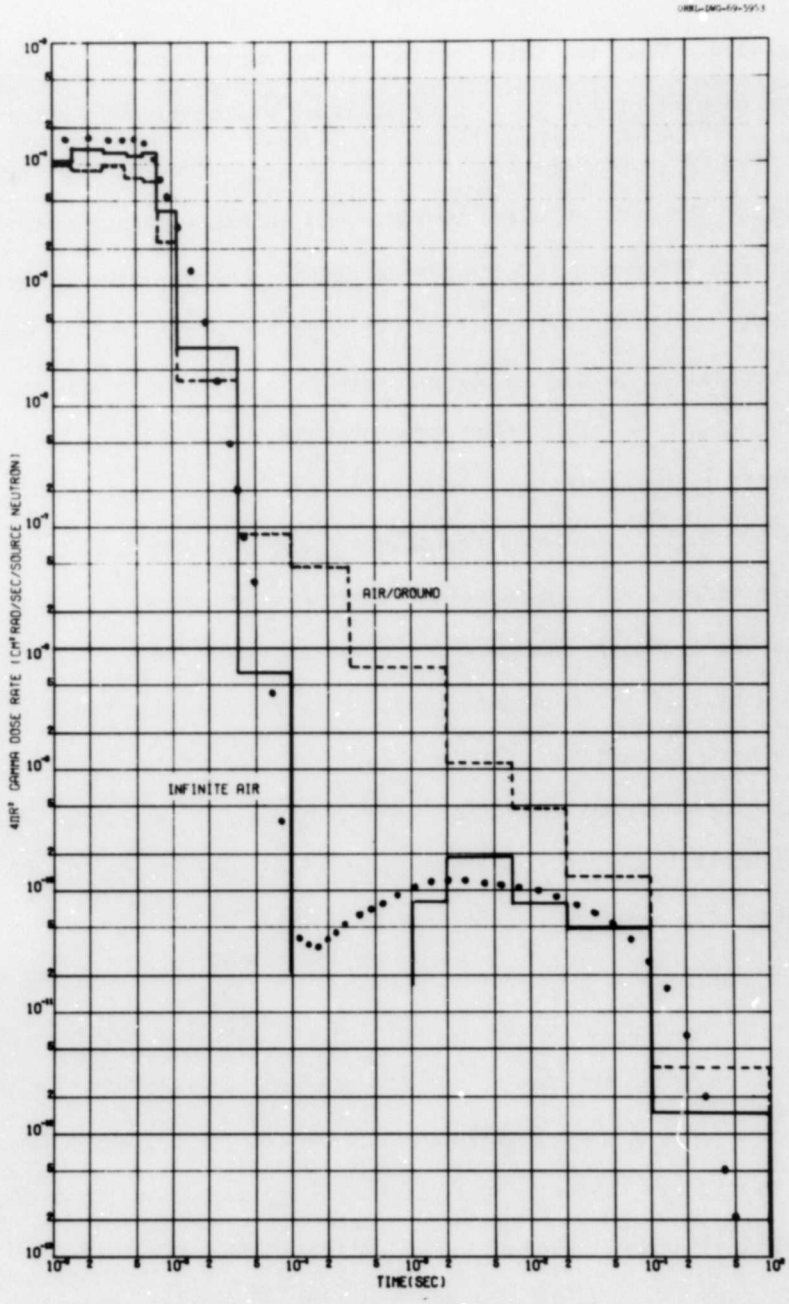

Fig. 19. Time Dependence of Secondary Gamma-Ray Dose Rate at 300 m Due to a 12.2- to 15-MeV Source. --- Air Over Ground for Source at 50 ft; —— Monte Carlo Results for Infinite Air; oooo Monte Carlo Results for Infinite Air Time-Dependent Discrete Ordinates.

sampling used. That is, this portion of the curve contains a small fraction of a percent of the total dose and thus was completely undersampled in the Monte Carlo calculation in which the importance sampling was set up to determine the dose rate due to fast- and thermal-neutron induced gamma rays, but not for gamma rays from intermediate energy neutron reactions. This clearly illustrates the effects of importance sampling on results that are not emphasized in the sampling scheme.

SUMMARY AND CONCLUSIONS

The effect of the ground on the secondary gamma-ray field is a stronger function of neutron source energy than of source height. To further illustrate this effect, Fig. 20 shows the fractional components of both capture and inelastic secondary gamma-ray dose versus range for a 12.2- to 15-MeV source. Note that the dominant component is the inelastic production in air. The next largest component, ≈10%, is thermal capture in the ground. It is therefore easy to understand why the secondary gamma-ray energy and angular distributions are not strongly affected by the ground since by far the largest components come from the air. For a fission source or a Godiva leakage spectrum, inelastic scatterings in the air and ground are less than 10% of the total, and the dominant contributors are from intermediate energy and thermal-neutron captures in the air and ground (Fig. 21). Thus the spatial variation of gamma-ray energy and angular distribution behaves more like the spatial variation of the thermal flux and not the fast flux.

To reiterate, the spatial, energy, and angular distribution of the fast-neutron radiation field can be reasonably approximated from results of infinite-air calculations using the techniques of French.[26] However, the ground has a significant effect on the variation of thermal flux, the secondary gamma-ray field, and the time dependence of these fields.

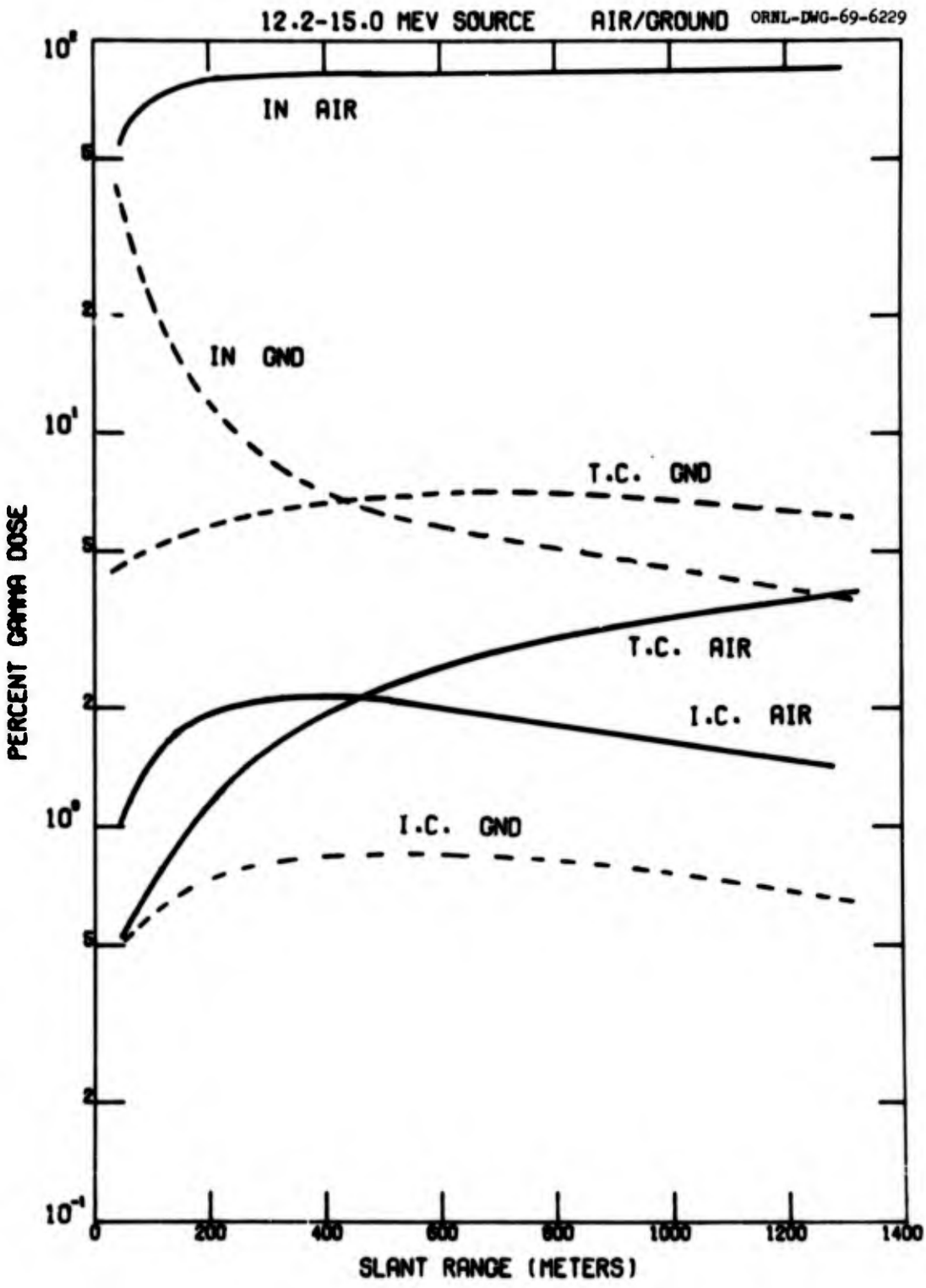

Fig. 20. Fractional components of Secondary Gamma-Ray Dose Due to a 12.2- to 15-MeV Neutron Source. IN ≡ Inelastics and Fast-Capture Gammas, I.C. ≡ Intermediate Captures (Neutrons with Energies Between 0.414 eV and 0.11 MeV), T.C. ≡ Thermal-Capture Gamma Rays. Source Height is 50 ft.

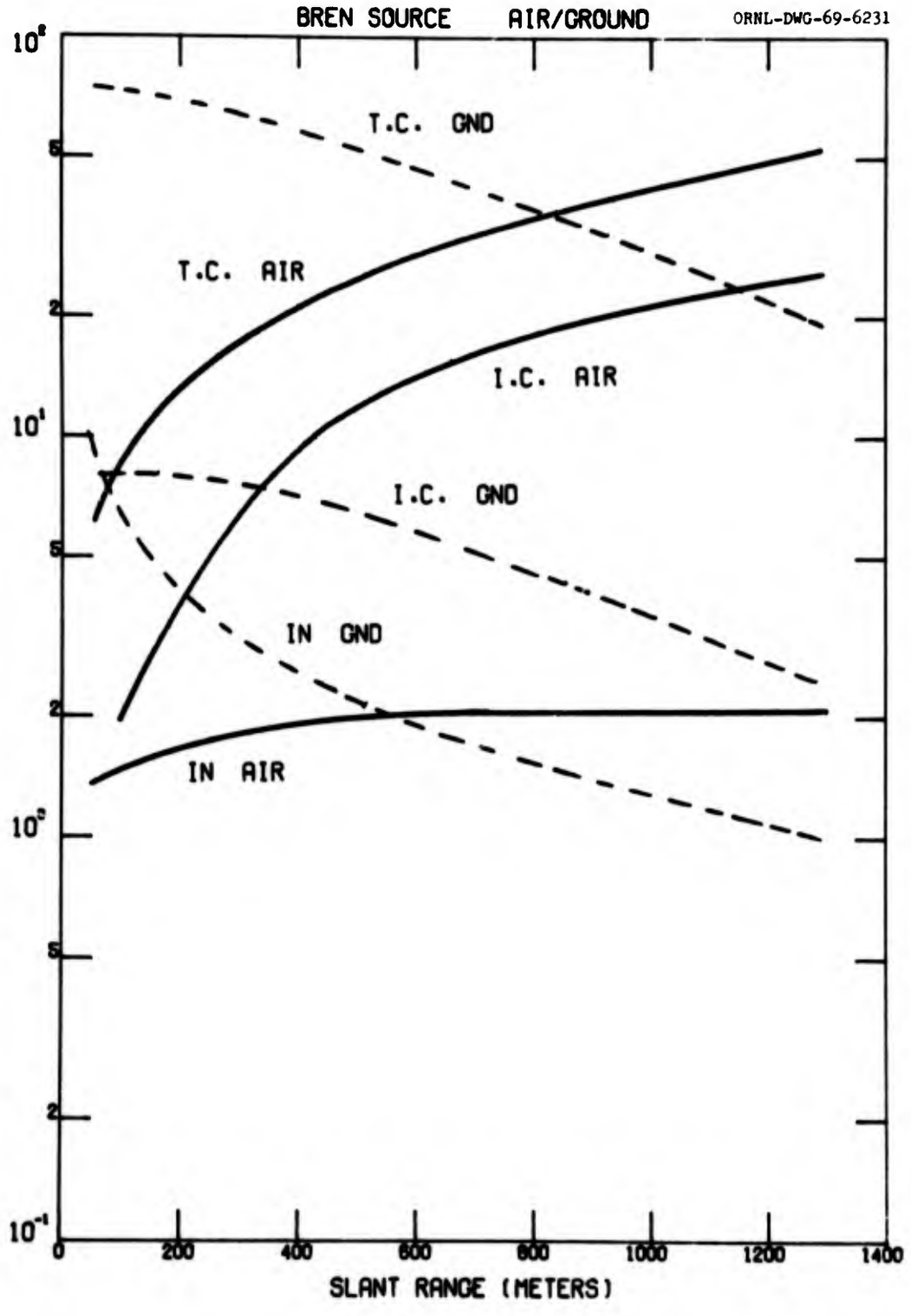

Fig. 21. Fractional Components of Secondary Gamma-Ray Dose Due to a Godiva Leakage Spectrum. IN ≡ Inelastic and Fast-Capture Gammas, I.C. ≡ Intermediate Capture (Neutrons with Energies Between 0.414 eV and 0.11 MeV), T.C. ≡ Thermal-Capture Gamma Rays. Source Height is 27 ft.

To properly determine these characteristics of the radiation field the air-ground interface must be included.

The description of the radiation field due to 9 source bands and several spectra has been determined for infinite air and for a source height of 50 ft. Additional calculations for a fission and 12.2- to 15-MeV source at a height of 1125 ft provide information on the effect of source heights. Also, results for detector heights above the ground permit a determination of the ground effect on the detector location. Thus the radiation field for sources from ground level up to approximately 20,000 to 30,000 ft has been determined.

ACKNOWLEDGMENTS

The author is indebted to many people who have been instrumental in various aspects of the work discussed. In particular, the development of the discrete ordinates techniques which were required for the problems were performed by F. R. Mynatt. R. J. Rodgers, M. L. Gritzner, and N. M. Greene were involved in the multigroup cross-section manipulations and the running of the discrete ordinates codes. In addition, the author is indebted to M. B. Emmett and C. L. Thompson for their efforts in modifying and running the Monte Carlo codes and in generating codes for editing, plotting, and combining results.

REFERENCES

1. D. C. Irving *et al.*, "05R, A General-Purpose Monte Carlo Neutron Transport Code," ORNL-3622 (1965).
2. S. K. Penny, D. K. Trubey, and M. B. Emmett,"OGRE, A Monte Carlo System for the Study of Gamma-Ray Transport, Including an Example (OGRE-P1) for Transmission Through Laminated Slabs," ORNL-3805 (1966).
3. V. R. Cain *et al.*, p. 92 in Neutron Physics Division Ann. Progr. Rept. for Period Ending May 31, 1967, ORNL-4134.
4. F. B. K. Kam and K. D. Franz, "ACTIFK, A General-Purpose Code to Analyze 05R Collision Tapes," ORNL-3856 (1966).
5. F. H. Clark, "The Exponential Transform as an Importance Sampling Device - A Review," ORNL-RSIC-14 (1966).
6. V. R. Cain, E. A. Straker, and G. Thayer, "Monte Carlo Path Length Selection Routines Based on Some Specific Forms of the Importance Function," ORNL-TM-1967 (1969).
7. F. H. Clark, "Variance of Certain Flux Estimators Used in Monte Carlo Calculations," Nucl. Sci. Eng. 27, 235 (1967).
8. W. W. Engle, "A User's Manual for ANISN - A One-Dimensional Discrete Ordinates Transport Code with Anisotropic Scattering," K-1693 (1967).
9. F. R. Mynatt, "A User's Manual for DOT - A Two-Dimensional Discrete Ordinates Transport Code with Anisotropic Scattering," K-1694 (to be published).
10. F. R. Mynatt, F. J. Muckenthaler, and P. N. Stevens, "Development of Two-Dimensional Discrete Ordinates Transport Theory for Radiation Shielding," CTC-INF-952 (1969).
11. D. C. Irving, 05R Cross Section Library Memo 2, Radiation Shielding Information Center ORNL Code Package CCC-17, 1965.
12. E. A. Straker, N. M. Greene, and R. J. Rodgers, "Calculations of Neutron Transport in the Atmosphere and the Effect of Input Cross Sections in a Review of the Discrete Ordinates S_n Method for Radiation Transport Calculations," ORNL-RSIC-19 (1968).
13. E. A. Straker, "Time-Dependent Neutron and Secondary Gamma-Ray Transport in an Air-Over-Ground Geometry. Vol. I. Calculational Techniques and Discussion of Results," ORNL-4289 (to be published).

14. J. K. Dickens and F. G. Perey, "The $^{14}N(n,x\gamma)$ Reaction for 5.8 $\leq E_n \leq$ 8.6 MeV," Nucl. Sci. Eng. 36, 280 (1969); also ORNL-TM-2778 (1969).
15. V. J. Orphan et al., "Neutron Cross-Section Data for Radiation Transport Calculations," GA-8006, Gulf General Atomic, Inc. (1969).
16. J. A. Auxier, F. F. Haywood, and L. W. Gilley, "General Correlative Studies - Operation BREN," USAEC Report CEX-62.03 (1963).
17. F. J. Muckenthaler et al., "An Evaluation of Simple Iron-Water Radiation Shields and Radiation Measurement Within Concrete-Lined and -Capped Pits," USAEC Report CEX-62.30 (1964).
18. F. F. Haywood, J. A. Auxier, and E. T. Loy, "An Experimental Investigation of the Spatial Distribution of Dose in an Air-Over-Ground Geometry," USAEC Report CEX-62.14 (1964).
19. "Operation Plans for Operation HENRE," USAEC Report CEX-65.03 (1965).
20. A. E. Fritzsche, N. E. Lorimier, and Z. G. Burson, "Measured High Altitude Neutron and Gamma-Dose Distributions Due to a 14-MeV Neutron Source," EGG-1183-1438 (1969).
21. A. E. Fritzsche, N. E. Lorimier, and Z. G. Burson, "Measured Low-Altitude Neutron and Gamma-Dose Distributions Due to a 14-MeV Neutron Source," EGG-1183-1449 (1969).
22. R. L. French and L. G. Mooney, "Prediction of Nuclear Weapon Neutron Radiation Environments," RRA-M92 (1969).
23. E. A. Straker, "Time-Dependent Neutron and Secondary Gamma-Ray Transport in an Air-Over-Ground Geometry. Vol. II. Tabulated Data," ORNL-4289, Vol. II (1968).
24. Radiation Shielding Information Center, Oak Ridge National Laboratory.
25. E. A. Straker and M. L. Gritzner, "Neutron and Secondary Gamma-Ray Transport in Infinite Homogeneous Air," ORNL-4464 (1969).
26. R. L. French, "A First-Last Collision Model of the Air/Ground Interface Effects on Fast-Neutron Distribution," Nucl. Sci. Eng. 19, 151 (1964).
27. W. W. Engle, F. R. Mynatt, and R. S. Booth, "One-Dimensional Time-Dependent Discrete Ordinates," ANS Trans. 12, 1 (1969).
28. Z. G. Burson,"Radiation Output Description From the $T(d,n)^4He$ Reaction in a Large Target (1000 cm^2) - Operation HENRE," USAEC Report CEX-65.04 (to be published).